The Joachim Dolomite : a Middle Ordovician sabkha of southeast Missouri and southern Illinois, USA

Autor(en): **Okhravi, Rasool / Carozzi, Albert V.**

Objekttyp: **Article**

Zeitschrift: **Archives des sciences et compte rendu des séances de la Société**

Band (Jahr): **36 (1983)**

Heft 3: **Archives de Science**

PDF erstellt am: **23.07.2024**

Persistenter Link: https://doi.org/10.5169/seals-740228

Arch. Sc. Genève	Vol. 36	Fasc. 3	pp. 373-424	1983

THE JOACHIM DOLOMITE: A MIDDLE ORDOVICIAN SABKHA OF SOUTHEAST MISSOURI AND SOUTHERN ILLINOIS, U.S.A.

BY

Rasool OKHRAVI and **Albert V. CAROZZI** [1]

ABSTRACT

The Joachim Dolomite (Middle Ordovician) was investigated in detail by means of 1154 samples collected from eleven stratigraphic sections located in southeast Missouri and southern Illinois.

Petrographic studies revealed eleven distinct carbonate-evaporite and clastic microfacies. From the superposition of the microfacies which form an ideal shallowing-upward sequence, a depositional-diagenetic model was constructed and demonstrated statistically. Its microfacies were interpreted in terms of depositional environments as follows: dolomitized pelletoidal calcilutite to calcisiltite (offshore); dolomitized mud-supported intraclastic calcarenite to calcirudite with calcisiltite matrix (shoreface); dolomitized grain-supported intraclastic calcarenite with interstitial pelletoidal calcisiltite matrix and poikilotopic sparite cement (intra-bioclastic bar); dolomitized mud-supported to grain-supported intraclastic pelletoidal calcarenite to calcirudite with calcisiltite matrix (back-bar flat); dolomitized pelletoidal calcilutite to calcisiltite (lagoon); dolomitized stromatolite-constructed limestone (stromatolitic ridge); dolomitized mud-supported to grain-supported oolitic-intraclastic calcarenite with calcisiltite matrix (oolitic flat); dolomitized stromatolite-bearing calcisiltite (carbonate flat); dolomitized pelletoidal calcisiltite with fenestral fabric (inner stromatolitic ridge); dolomitized calcilutite with anhydrite and gypsum (evaporitic flat); pure quartz arenite (dunes). Unimodal and bimodal quartz arenites deposited respectively in dune and interdune positions by winds were taken as an independent evidence to demonstrate the desert environment and its temporary extension over the carbonate domain.

The offshore through lagoonal microfacies were secondarily dolomitized by a freshwater-seawater mixing process (Dorag model), while the rest of the microfacies were dolomitized penecontemporaneously by an evaporative pumping mechanism of sabkha type.

The general environmental evolution of the microfacies shows that a complete section of the Joachim Dolomite consists of the superposition of eleven asymmetric cycles which display a slow shallowing-upward phase followed by a rapid deepening phase.

Paleoclimatic data confirm that the investigated area was located during the Middle Ordovician at the appropriate latitude for development of an arid climate and that the Joachim Dolomite can be interpreted as a large-scale sabkha covering the southern part of Illinois with a transition to open sea conditions in a southward direction.

[1] Department of Geology, University of Illinois at Urbana-Champaign, Urbana, Illinois, 61801, U.S.A. This paper is part of a doctoral dissertation completed by R. O. under the supervision of A.V.C. and submitted to the Graduate College in November 1982.

This research was partially supported by a grant from Petróleo Brasileiro S.A. PETROBRAS which is gratefully acknowledged. The Illinois State Geological Survey is thanked for generously providing the core samples.

RÉSUMÉ

La dolomie de Joachim (Ordovicien moyen) a été étudiée au moyen de 1154 échantillons représentant onze coupes stratigraphiques distribuées dans le sud-est du Missouri et le sud de l'Illinois.

Les études pétrographiques ont révélé la présence de onze microfaciès carbonato-évaporitiques et clastiques. A partir de leur superposition qui forme une série idéale de profondeur décroissante, un modèle dépositionel-diagénétique a été construit et vérifié par des méthodes statistiques. Ses microfaciès ont été interprétés au point de vue des conditions de dépôt comme suit: calcilutite à calcisiltite pelletoidale dolomitisée (mer ouverte); calcarénite à calcirudite intraclastique dolomitisée à grains non jointifs et à matrice calcisiltique (avant-plage); calcarénite intraclastique dolomitisée à grains jointifs avec matrice calcisiltique pelletoidale et ciment de sparite poikilotopique (barre intra-bioclastique); calcarénite à calcirudite dolomitisée à grains non jointifs à jointifs et à matrice calcisiltique (platier d'arrière-barre); calcilutite à calcisiltite pelletoidale dolomitisée (lagune); calcaire construit dolomitisé à stromatolites (crête stromatolitique); calcarénite oolithique — intraclastique dolomitisée à grains non jointifs à jointifs et à matrice calcisiltique (platier oolithique); calcisiltite à stromatolites dolomitisée (platier carbonaté); calcisiltite pelletoidale dolomitisée à texture fenestrale (crête stromatolitique interne); calcilutite dolomitisée à anhydrite et gypse (platier évaporitique); grès quartzeux purs (dunes). Les grès quartzeux unimodaux et bimodaux de la dolomie de Joachim déposés respectivement en position de dune et d'interdune ont été utilisés comme données indépendantes pour démontrer le milieu désertique et ses invasions temporaires du domaine carbonaté.

Les microfacies qui s'étendent du domaine de mer ouverte à lagunaire ont été dolomitisés par un processus diagénétique de mélange d'eau douce et salée (modèle Dorag), tandis que les autres microfaciès ont été dolomitisés de manière pénécontemporaine par un mécanisme de pompage évaporatif de type sabkha.

L'évolution générale des microfaciès au point de vue du milieu de dépôt montre qu'une coupe complète de la dolomie de Joachim résulte de la superposition de onze cycles asymétriques qui montrent une phase lente de diminution de profondeur suivie par une phase d'augmentation rapide.

Les données paléoclimatiques confirment que la région étudiée se trouvait pendant l'Ordovicien moyen à une latitude correspondant à un climat aride et que la dolomie de Joachim peut être interprétée comme une sabkha de grande extension couvrant la partie méridionale de l'Illinois avec une transition à la mer ouverte vers le sud.

INTRODUCTION

The purpose of this study lies in the following areas: detailed petrographic investigation of the Joachim Dolomite in order to define the microfacies forming its different members; environmental interpretation of the microfacies leading to a depositional-diagenetic model; determination of the processes of dolomitization; interpretation of the small scale cyclicity of the microfacies and of the general evolution of the depositional environments of the Joachim Dolomite.

REVIEW OF PREVIOUS WORK

In their important work Templeton and Willman (1963) subdivided the Joachim Dolomite in southeast Missouri and southwest Illinois into six members (Figure 1) on the basis of variations in content of shale, silt, and sand and differences in bedding.

They carefully established the lateral relationships and superposition of the members section by section in the field. These sections (A, B, C, D, and G) were resampled for this microfacies study. Templeton and Willman also determined the spatial

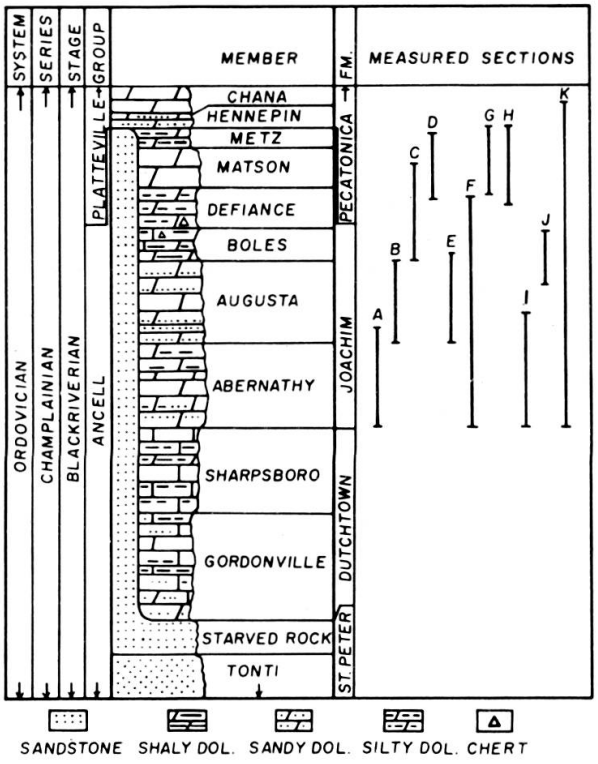

FIG. 1. — Columnar section of the Joachim Dolomite (after Templeton and Willman, 1963).

relationships between the Joachim Dolomite and the adjacent formations as follows: in southern Illinois, the Joachim and Dutchtown strata overlie the Starved Rock Member of the St. Peter Sandstone, while in northern Illinois, north of a line extending from Chicago to Quincy the Starved Rock Sandstone is overlain by the Glenwood Formation. The Glenwood, Dutchtown, and Joachim Formations all appear to be in facies relationship with the upper part (Starved Rock Member) of the St. Peter Sandstone. No terminology changes were suggested in the handbook of Illinois stratigraphy (Willman *et al.*, 1975). Thacker and Satterfield (1978) described some new Joachim outcrops on roadcuts along Interstate-55 in southeast Missouri, of which two (sections F and I) were selected for sampling in this study.

The earliest petrographic report on the Joachim Dolomite was by Freeman (1966a). He studied the Ordovician rocks including some Joachim outcrops in northern Arkansas. He observed some channeling at the contact of the Joachim and the overlying basal Plattin beds and compaction of the latter over local highs. He considered these features as indicating an episode of widespread subaerial erosion.

Freeman (1965 [abs.], 1966b) interpreted the dolomite of the Joachim as post-lithification. Young *et al.*, (1972) studied carbonate facies in the Ordovician rocks (including the Joachim) of northern Arkansas and concluded that the formational contact between the Joachim Dolomite and the Plattin Limestone was caused by regional facies shifts and not by subaerial exposure and erosion as suggested by Freeman (1966a). They interpreted the Joachim Dolomite as deposited in an intertidal to supratidal environment. Handford and Moore (1976) developed a depositional-diagenetic model to interpret the formation of hopper-shaped calcite pseudomorphs after halite occurring in the Joachim Dolomite of northern Arkansas. They concluded that the halite grew within the sediments from upward moving phreatic marine water through an evaporative pumping mechanism.

The possibility of the Joachim Dolomite being of economic interest and providing both a reservoir and an anhydrite cap for hydrocarbon accumulation was mentioned by Sloss (1970). According to him, the combination of the Joachim Dolomite and of the underlying Dutchtown Limestone in any prograding and regressive sequence could provide a stratigraphic trap for hydrocarbon accumulation. The Dutchtown Limestone consists of a considerable thickness of dark, fetid, clay-rich carbonates that probably represent a deep, poorly oxygenated marine basin. The Joachim Dolomite with its light colored complex of algal and micritic dolomite with a varying content of clay and silt, marked by mud cracks and other evidence of shallow-water deposition, represents the margin of the basin. Intertonguing of the basin-margin deposits and the organic rich, basin-interior muds would establish the conditions necessary for the development of permeable, dolomitized algal banks with impermeable source beds above and below, sealed up-dip by lagoonal or supratidal anhydrite.

METHODS OF STUDY

Sampling techniques and localities

Eleven stratigraphic sections (Figure 2) were selected for this study (Okhravi, 1982) among which ten (A through J) are exposures of the various members on the flanks of the Ozark Dome in southeast Missouri and southwest Illinois, and one (K) is the core of well Superior Oil C-17 Ford, White County, southeast Illinois in the central part of the Illinois Basin. This core, kindly provided by the Illinois State Geological Survey, is a complete section of the Joachim Dolomite (61 meters thick) overlying the Dutchtown Limestone and overlain by the Platteville Group.

A total of 1154 carbonate (vertically oriented) and shale samples were collected. Among them 915 samples were obtained from outcrops, with an average sampling interval of 11 cm and the rest from the core with a sampling interval of 30.5 cm.

MICROFACIES ANALYSIS

Thin sections were prepared from all carbonate samples, they were stained with alizarin red S and potassium ferricyanide solution following the staining method proposed by Dickson (unpublished, 1980) and slightly modified (Okhravi, 1982). The advantage of this method is its capability to stain six different carbonate minerals (calcite, ferroan calcite, dolomite, ferroan dolomite, rhodocrosite and aragonite).

Thin sections were visually subdivided into microfacies on the basis of their petrographic properties such as textures, grain size, biota, proportion of micrite matrix to sparite cement, etc. They were then studied following the microfacies technique proposed by Carozzi (1958 and 1961), and expanded with his coworkers (Stricker and Carozzi, 1973; Kuhnhenn and Carozzi, 1977; Carozzi and Diaby, 1982). It consists of tabulating the indices of clasticity and frequency of all inorganic and organic detrital components, and the frequency of all benthic and planktic organic components (whole or broken) of a carbonate rock. The index of clasticity

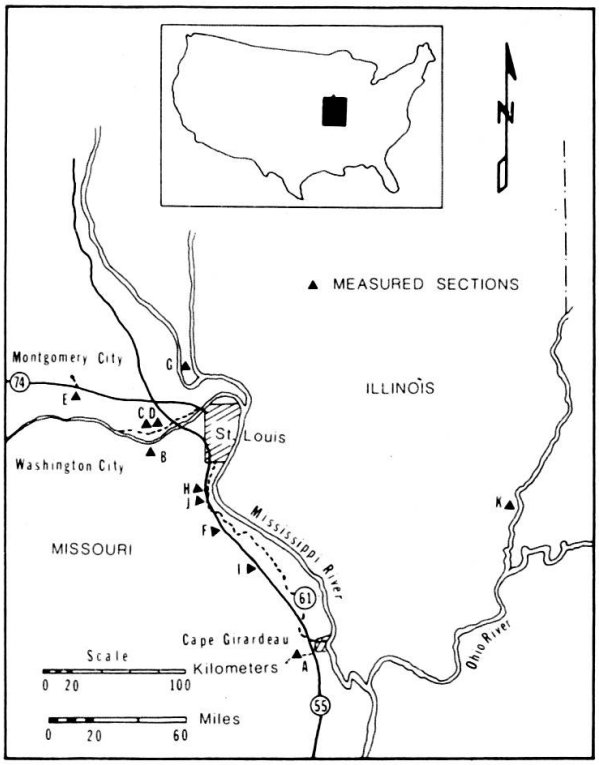

FIG. 2. — Location map.

was obtained by averaging the diameter of the six largest, subequal grains in each one of six fields on a particular thin section. The frequency index of all components except pellets and fine quartz was determined over a standard surface area of 230.8 sq mm consisting of six juxtaposed field surfaces of the thin section and the

total of the six fields was considered the frequency of the component. A total surface area of 38.46 sq mm was used for pellets and fine quartz.

In addition to frequency and clasticity measurements the relative abundance of other features that could not be statistically measured or of minor components which are important for environmental interpretation were visually estimated and expressed by rare (<1%), present (1-5%), common (5-10%), and abundant (>10%).

Due to the fact that the Joachim Dolomite consists of non-particulate constituents such as anhydrite, dolomite, stromatolite, etc. as well as particulate components, the frequency of all constituents was also estimated in percent surface area. Therefore the same statistical analysis could cover all types of components.

The intensity of dolomitization was defined as the total dolomitized surface area measured in percent over a standard surface of 230.8 sq mm. The following terminology and crystal size (Folk, 1962) were used to characterize dolomite rhombs and hence express the crystallinity of dolomite.

Extremely coarsely crystalline	>4 mm
Very coarsely crystalline	1-4 mm
Coarsely crystalline	0.25-1 mm
Medium crystalline	0.062-0.25 mm
Finely crystalline	0.016-0.062 mm
Very finely crystalline	0.004-0.016 mm
Aphanocrystalline	<0.004 mm

Upon completion of all the microscopic measurements the microfacies were classified a second time on the basis of frequency, clasticity, and percent surface area.

Statistical analysis

The validity of the classification of microfacies was evaluated using a multivariate classification program (ITERIM) written by Demirmen (1969). After the interations had stabilized the "rejected" thin sections were reexamined to determine if the "computer classification" was geologically significant and hence to be taken into account. Since the computer classification is entirely based on quantitative data and does not take into account the qualitative to semi-quantitative parameters pertaining to sedimentary structures, textures, etc., the computer classification could not always be accepted. For instance, offshore micrites (microfacies 1) could not be discriminated from lagoonal micrites (microfacies 5). The average value of the measured parameters for each microfacies were calculated using the SOUPAC statistical package (Tables 1 and 2).

The interrelationships between the microfacies are established in two manners, first by bivariate correlation analysis using the SOUPAC statistical subroutine

TABLE 1

Average Values of Components by Microfacies

Components	MICROFACIES 1	2	3	4	5	6	7	8	9	10	11
Pelmatozoan freq.	6.6	----	----	----	----	----	----	----	----	----	----
Ostracode freq.	14.4	13.8	34.2	9.6	7.2	0.6	----	----	----	----	----
Nuia freq.	93.6	6.0	----	----	----	----	----	----	----	----	----
Stromatolite mats %	----	----	----	1.2	1.6	23.8	7.9	1.4	2.0	0.1	----
Oncolite freq.	----	----	248.4	3.6	----	----	----	----	----	----	----
Oncolite clast.	----	----	0.468	0.038	----	----	----	----	----	----	----
Bioturb. intensity %	2.4	4.0	1.2	0.8	12.4	2.5	----	0.9	----	0.1	----
Pellet freq.	82.3	----	115.8	350.8	5.4	85.1	4.2	72.6	471.2	1.0	----
Pellet clast.	0.007	----	0.068	0.044	0.010	0.002	0.022	0.017	0.023	0.014	----
Intraclast 1 freq.	----	132.6	28.8	----	----	----	----	----	----	----	----
Intraclast 1 clast.	----	0.605	0.114	----	----	----	----	----	----	----	----
Intraclast 2 freq.	----	----	271.2	403.8	17.4	4.8	94.8	60.0	31.2	6.0	----
Intraclast 2 clast.	----	----	0.600	0.440	0.122	0.100	0.580	0.166	0.242	0.140	----
Oolite(sup.) freq.	----	----	----	----	----	----	1047	----	----	----	----
Oolite(sup.) size	----	----	----	----	----	----	0.261	----	----	----	----
Coarse quartz freq.	----	----	37.2	106.8	36.6	----	142.8	653.6	650.4	0.6	526.8
Coarse quartz clast.	----	----	0.090	0.074	0.405	----	0.021	0.475	0.435	0.200	0.480
Fine quartz freq.	----	----	10.2	188.8	381.1	19.6	66.2	814.8	543.9	7.4	1167.8
Fine quartz clast.	----	----	0.022	0.049	0.076	0.013	0.018	0.094	0.073	0.008	0.099
Intensity of dol. %	59.3	53.2	28.0	58.3	55.8	72.1	60.0	64.0	42.7	50.5	5.0
Dolomite rhomb size	0.062	0.064	0.037	0.028	0.030	0.025	0.037	0.029	0.017	0.022	0.015
Evaporite %	----	----	0.4	2.6	1.4	3.6	0.5	2.6	3.0	40.2	2.0
Pyrite %	0.1	----	----	0.6	0.7	0.3	----	0.4	----	1.1	----
Pyrite Xl. size	0.002	----	----	0.006	0.006	0.007	----	0.002	----	0.011	----
Authigenic silica f	----	----	----	42.0	8.4	40.8	----	9.0	18.0	6.6	----
Authigenic s. Xl. s.	----	----	----	0.008	0.006	0.015	----	0.004	0.016	0.006	----

TABLE 2

Average Percent Surface Area Covered by each Component or Constituent

Component or Constituent	MICROFACIES 1	2	3	4	5	6	7	8	9	10
Pelmatozoan	1.2	0.0	0.0	0.0	0.0	0.0	0.0	0.0	0.0	0.0
Ostracode	2.0	3.8	0.0	20.0	0.7	1.2	0.7	0.2	0.2	0.0
Nuia	1.6	0.1	0.0	0.0	0.0	0.0	0.0	0.0	0.0	0.0
Stromatolite mats	0.0	0.0	0.0	1.5	1.4	23.4	7.9	1.3	0.4	0.1
Oncolite	0.0	0.0	18.4	0.8	0.0	0.0	0.0	0.0	0.0	0.0
Bioturb. Intensity	2.4	4.0	0.0	1.0	12.3	2.6	0.0	0.8	0.0	0.1
Pellet	1.0	0.0	4.9	9.7	0.3	0.5	4.1	1.1	11.4	0.3
Intraclast 1	0.0	15.4	4.0	0.0	0.0	0.0	0.0	0.0	0.0	0.0
Intraclast 2	0.0	0.0	11.4	14.8	1.0	0.6	6.2	1.7	0.0	0.0
Superficial Oolite	0.0	0.0	0.0	0.0	0.0	0.0	30.4	0.1	0.0	0.0
Dolomite matrix	59.4	51.8	19.5	39.3	55.8	56.1	28.7	64.1	29.7	50.4
Evaporite	0.0	0.0	0.4	2.5	1.4	3.6	0.6	2.4	3.0	39.5
Pyrite	0.0	0.0	0.0	0.6	0.7	0.3	0.0	0.4	0.0	1.1
Fenestral Fabric	0.0	0.0	0.0	0.1	0.0	0.3	0.0	0.1	14.5	0.0

(SOUPAC, 1976), second by studying the vertical superposition of the microfacies which form the shallowing-upward sequences. The combination of these techniques leads to a vertical ideal cycle of the various microfacies which is then interpreted horizontally as a depositional model according to Walther's rule (1894, in Middleton, 1973).

COMPONENTS

Because of the difficulty in identifying and counting skeletal debris below 60 microns by means of a conventional petrographic microscope, this boundary value was used as limit between grains and matrix.

Major organic components

Ostracodes and blue-green algae are the most abundant organisms. Ostracodes are mostly large *Leperditia* associated with small ones. Blue-green algae in the form of laminated and labyrinthic colonies (Spongiostromata) form stromatolitic mats, encrustations as well as oncolites.

Minor organic components

Nuia, gastropods, *Lingula*, and trilobites in decreasing order of importance constitute the minor organic components.

Inorganic Components and Constituents

Bimodal quartz grains with fine mode ranging from 0.02 to 0.20 mm and coarse mode ranging from 0.25 to 0.80 mm are the most common inorganic component. Pellets are mainly lithic in origin ranging from angular to rounded, however, some fecal pellets with uniform size and rounded shape are present. The arbitrary cut-off point of 0.15 mm (Folk, 1962) was used to separate lithic pellets from intraclasts. Intraclasts are of two different kinds, intraclasts 1 and intraclasts 2. The former consist of partially dolomitized micrite of relatively deeper water with *Nuia* and ostracode fragments, while the latter consist mostly of finely crystalline dolomitized lagoonal micrite resulting mainly from desiccation of micrite and intraformational reworking. Superficial ooids ranging from spastolites to non-deformed types are present. Detrital grains of anhydrite and gypsum occur only in core samples. Minor diagenetic components are pyrite crystals, authigenic quartz and authigenic K-feldspar.

Bedded, nodular, crystal shaped, and massive anhydrite, as well as gypsum are the main evaporitic constituents. Halite is present in small amount and preserved only as cubical casts within carbonates.

DESCRIPTION OF MICROFACIES

The petrographic study led to the distinction of eleven microfacies which have been secondarily dolomitized to a variable degree. In order to avoid confusion between depositional and diagenetic features the microfacies are designated and described as they were originally deposited. The microfacies were dolomitized by means of two different processes: freshwater-seawater mixing or Dorag model (Badiozamani, 1973) and evaporative pumping under sabkha conditions (Hsü and Siegenthaler, 1969). Microfacies 1 through 5 were mainly dolomitized by the first process, while microfacies 6 to 11 were dolomitized by the second. The porosity type(s) which existed or exist today in each microfacies are designated according to the terminology proposed by Choquette and Pray (1970). The microfacies are numbered starting from the marine environment and in the direction of the continent according to the depositional model to be described later.

Microfacies 1

Dolomitized pelletoidal calcilutite to calcisiltite with up to 10% scattered sand-size bioclasts of large ostracodes, pelmatozoan and *Nuia* (Plate 1, A and B). Bioturbation is extensive and represented by borings and burrows filled by sparite cement or coarser matrix.

Dolomitization is patchy and varies between 20%-80% with an average of 59.3%. It is characterized by equal size medium crystalline rhombs (Plate 1, B) replacing the matrix and partially the bioclasts.

Environmental interpretation: subtidal, low energy.

Microfacies 2

Dolomitized mud-supported intraclastic calcarenite to calcirudite with few bioclasts and calcisiltite matrix (Plate 1, C and D). The intraclasts are poorly sorted, angular to subrounded and reworked from early cemented microfacies 1. Some of the intraclasts are composite indicating at least two episodes of intraformational reworking (Plate 1, D). Bioclasts are large ostracodes and a few *Nuia*.

Dolomitization is limited to the micrite matrix (53.2%) and characterized by medium euhedral rhombs as in microfacies 1.

Environmental interpretation: subtidal, low to medium energy, reworked.

Microfacies 3

Dolomitized grain-supported intraclastic biocalcarenite with interstitial pelletoidal calcisiltite matrix and poikilotopic sparite cement (Plate 1, E and F). The intraclasts are mostly rounded and originated from reworking of early cemented micro-

facies 1 and 2. The bioclasts are mostly ostracodes encrusted by blue-green algae. Whenever oncolites occur, they are neomorphosed or poorly defined. Grains of detrital quartz marginally replaced by calcite (now dolomite) are present.

Two generations of cement can be recognized which indicate the following time relation:

1. Development of vuggy porosity by early submarine dissolution (Plate 1, E).
2. Precipitation of beachrock or submarine isopachous rim cement probably aragonite or high-Mg calcite on the walls of vugs and of preexisting interparticle pore spaces.
3. Complete dolomitization of rim cement, and partial dolomitization of interstitial matrix, intraclasts and bioclasts.
4. Sequence of vadose and phreatic diagenetic conditions characterized by influx of vadose silt and precipitation of poikilotopic sparite cement which obliterated the porosity.

Dolomitization (28%) is the least extensive of all the carbonate microfacies and characterized by finely euhedral rhombs partially replacing the intraclasts and bioclasts. The main fabric selective porosity was interparticle.

Environmental interpretation: low intertidal, medium energy, reworked.

Microfacies 4

Dolomitized mud-supported to grain-supported intraclastic pelletoidal calcarenite to calcirudite with calcisiltite matrix (Plate 1, G and H). Intraclasts are poorly sorted and range from angular to rounded and appear to be reworked desiccation chips of micrite (Plate 1, G). Pellets are lithic in origin and result from disintegration of the desiccation chips. Bioclasts ranging up to 7 percent are mainly ostracodes. Bimodal quartz grains occasionally occur with marginal replacement by micrite. Detrital anhydrite is present only in the core samples. Bioturbation is characterized by the circular arrangement of sand size particles in the matrix.

Interparticle pores are filled by vadose silt and poikilotopic sparite cement. Dolomitization (58.3%) is more extensive than in microfacies 3. Intraclasts and matrix are partially dolomitized. Dolomite is characterized by very fine to fine subhedral to euhedral rhombs. The dominant porosity type was interparticle.

Environmental interpretation: intertidal, medium energy, periodically exposed, desiccated.

Microfacies 5

Dolomitized pelletoidal calcilutite to calcisiltite with up to 10% bioclasts of *Leperditia*, and a small number of gastropods and *Lingula*. Bimodal quartz grains with intensive marginal replacement by micrite occur occasionally. Pellets

are mainly lithic in origin with few fecal ones. The high intensity of bioturbation is shown by vertical, horizontal, oblique, L-shaped borings and burrows (Plate 2, A and B). Borings are either empty now (porosity), or filled by matrix and/or cavity filling poikilotopic sparite cement showing geopetal features. Some of these borings (Plate 2, A) show the following depositional-diagenetic time sequence:

1. Early submarine lithification of the substratum.
2. Boring of the substratum by scavengers and development of non-fabric selective porosity.
3. Precipitation of probably aragonite or high-Mg calcite isopachous rim cement.
4. Complete dolomitization of the rim cement, partial dolomitization of interstitial matrix, pellets and bioclasts.
5. Influx of vadose silt.
6. Obliteration of the porosity by precipitation of cavity filling freshwater phreatic sparite cement.

Dolomitization is extensive (55.8%) throughout this microfacies and both matrix and grains (if any) are dolomitized. Dolomite is characterized by very fine to fine euhedral to subhedral rhombs. The only fabric selective porosity was intercrystalline, while other types of non-fabric selective porosity were borings, burrows, and vugs. Some of the borings and vugs are not filled (porous now).

Environmental interpretation: subtidal, low energy.

Microfacies 6

Dolomitized stromatolite-constructed limestone with occasional fenestral fabric. The stromatolites consist of dark superposed mats interbedded with biocalcisiltite laminae which contain large ostracodes (Plate 2, C and D). Molds of gypsum and anhydrite crystals and euhedral authigenic quartz are developed within the algal mats. Desiccation cracks and breccias, exposure crusts, and vadose silt are common. Desiccation cracks and fenestrae are filled by poikilotopic sparite cement.

Dolomitization is the most extensive (72.1%) of all the microfacies. The algal mats are dolomitized by very fine to fine subhedral rhombs. The calcisiltite groundmass has been changed to either ferroan dolomite or dolomite. Borings, burrows, molds of anhydrite crystals, and fenestral were the dominant types of porosity, some of which have been preserved.

Environmental interpretation: intertidal, low to medium energy, periodically exposed.

Microfacies 7

Dolomitized mud-supported to grain-supported oolitic-intraclastic calcarenite with matrix of calcisiltite interbedded with dark, thin stromatolitic mats. Superficial ooids appear as oomoldic pores, or are filled by poikilotopic sparite cement (Plate 2, E), secondary gypsum and quartz. Few ooids retain their original pelletoidal core. Some ooids show little or no deformation while others are spastolites resulting from strong deformation due to compaction followed by dolomitization and dissolution of their cores (Plate 2, F). Few rounded intraclasts of stromatolitic micrite are scattered among the ooids. Detrital quartz is present.

The matrix and the thin cortex of the ooids are dolomitized. Dolomite (60%) is characterized by fine subhedral to euhedral rhombs. The dominant porosity type now is oomoldic but a few of the moldic pores have been filled.

Environmental interpretation: intertidal, low energy.

Microfacies 8

Alternating dolomitized poorly developed dark organic-rich stromatolitic mats and light colored laminae of calcisiltite with bimodal quartz grains (Plate 2, G). Bimodal quartz grains with replaced edges appear occasionally as well as isolated molds of gypsum and anhydrite.

Dolomite (64%) is characterized by fine subhedral to euhedral rhombs becoming in places coarsely crystalline. Authigenic quartz and K-feldspar with euhedral crystals are present. Many samples of this microfacies are brecciated forming collapse breccias indicating dissolution of associated salt (Plate 2, H). Vadose silt and cavity filling calcite cement are present in the brecciated samples filling the cracks (Plate 2, H). Some late diagenetic dolomite rhombs floating in cavity filling sparite cement have been found in some of the samples of this microfacies. The growth of these rhombs postdates the precipitation of the sparite cement. The dominant porosity types were vuggy, channel, and moldic.

Environmental interpretation: high intertidal, low energy, exposed, associated with mud cracks.

Microfacies 9

Dolomitized pelletoidal calcisiltite with fenestral fabric, scattered bimodal quartz grains (Plate 3, A), and intercalated stromatolitic mats with desiccation and fracturation textures. Few hopper-shaped salt casts are preserved (now) as moldic porosity (Plate 3, B). Fenestrae are filled by vadose silt, and poikilotopic sparite cement. This microfacies grades in places into a dolomitized flat-pebble conglomerate (tempestite) with a matrix of pelletoidal calcisiltite or association of pelletoidal

calcisiltite and cavity filling sparite cement (Plate 3, C). The pebbles consist of poorly-sorted, subangular to rounded reworked desiccation chips of microfacies 6 and 8.

Both grains and matrix are dolomitized. The dolomite (42.7%) is characterized by fine subhedral rhombs. The dominant porosity type was fenestral.

Environmental interpretation: high intertidal to supratidal, tempestite.

Microfacies 10

Dolomitized calcilutite with anhydrite and gypsum, and occasional supply of bimodal quartz grains (Plate 3, D, E and H). The occurrence of evaporite in the outcrop samples is inferred from the moldic porosity left after dissolution of anhydrite crystals, and from pseudomorphs of calcite after anhydrite (Plate 3, D and H), although a few outcrop samples with preserved gypsum have been found. In most cases the anhydrite molds have been filled by vadose silt and poikilotopic sparite cement. The types of anhydrite of this microfacies were classified by using two basic properties, structure and texture, as described by Maiklem *et al.*, (1969). External form (presence or absence of crystal shape), anhydrite to matrix relationship, bedding, and distortion were used for structural analysis. Size, shape, and spatial relationship of crystals within the anhydrite masses were used for textural analysis. There are 5 types of anhydrite in this microfacies which are as follows: crystal shaped; nodular; nodular-mosaic; mosaic; massive.

Crystal-shaped anhydrite is either equidimensional with crystal size >0.06 mm or elongate. The elongate crystals are divided into two groups on the basis of crystal size, <0.5 mm, and >0.5 mm. They are randomly oriented or aligned and cluster spatial relation is rare. Nodular anhydrite consists of irregularly-shaped masses of anhydrite which are equidimensional and separated from one another by matrix. They are mostly lined up parallel to bedding or distorted. Bedded nodular anhydrite shows parallel, discontinuous, and even or wavy bedding. It ranges from distorted to non-distorted. Nodular-mosaic anhydrite forms masses which are equidimensional and partly coalescent. It is similar to nodular anhydrite with respect to bedding and distortion. Mosaic anhydrite ("chickenwire" structure) consists of coalesced anhydrite masses which are approximately equidimensional with little or no matrix. They are variably distorted and bedded with parallel, discontinuous, and even or wavy bedding. Massive anhydrite is mostly bedded with parallel, even, and wavy or curved bedding. In some cases it consists of many small acicular crystals. In core samples, the anhydrite also occurs as cavity filling cement in cracks of the collapse breccias.

Dolomite (50.5%) occurs mostly as matrix and as replacement of anhydrite. It is characterized by fine euhedral rhombs. The main porosity type was moldic, and has been preserved in a few samples.

Environmental interpretation: supratidal, coastal sabkha, evaporitic flat.

MICROFACIES 11

Bimodal quartz arenite with matrix of sericite and quartz or quartz overgrowth, or poikilotopic sparite cement, or association of dolomite and anhydrite cement (Plate 3, F and G). It consists of very well rounded grains of quartz with up to 10 percent K-feldspar and occasional grains of tourmaline. The diameter ratio of the two modes ranges up to 8:1, with very few grains of intermediate size. Typically the bimodal quartz arenite is a mixture of medium sand with fine to very fine sand with size range of 0.25 to 0.80 mm (coarse mode) and of 0.02 to 0.20 mm (fine mode). Each mode has excellent sorting within itself, yet the arenite has "poor" overall sorting. In many specimens the fine grains are in majority and the coarser grains scattered in a groundmass of finer ones, others consist of unimodal grains of almost uniform grain size (Plate 3, G).

Carbonate cements in the form of poikilotopic calcite and dolomite are common. Where the calcite or dolomite cement is present marginal replacement of quartz is observable. In core samples an association of anhydrite and dolomite cement is present in which the former has been partially replaced by the latter. Where carbonate cement or matrix are absent the original primary interparticle porosity has been reduced by quartz and feldspar overgrowths (Plate 3, G). Dolomite (5%) is present only as cement, and characterized by fine to medium euhedral rhombs. The main porosity type was reduced interparticle which has been preserved in a few samples.

Environmental interpretation: continental sabkha, eolian (dunes).

DEPOSITIONAL-DIAGENETIC MODEL

TECHNIQUES

The depositional-diagenetic model, as mentioned earlier, is constructed by means of two approaches: a bivariate correlation analysis between microfacies, and a detailed stratigraphic analysis of the superposition of the microfacies which build shallowing-upward sequences. Both approaches confirm each other and reveal a complete vertical sequence of eleven distinct microfacies.

The correlation coefficients of the carbonate microfacies by component means (Table 3) shows the high degree of correlation between successive microfacies. This condition also exists between microfacies 1, 5 and 8 due to the fact that they all consist of micrite and could not be discriminated by the computer program. They were separated therefore from each other by means of petrographic criteria. Similarly, the sequential position of microfacies 11, bimodal quartz arenite, mostly deposited by eolian processes rather than hydrodynamic forces was established by detailed stratigraphic analysis since it could not be treated by computer techniques. This is also true for the bimodal quartz grains which occur in some carbonate micro-

TABLE 3

Correlation Coefficients of Carbonate Microfacies by Component Means

Microfacies	1	2	3	4	5	6	7	8	9	10
1	1.00000									
2	.91026	1.00000								
3	.53669	.50708	1.00000							
4	.92238	.84027	.56996	1.00000						
5	.93448	.94773	.47442	.88330	1.00000					
6	.88045	.83927	.39212	.82138	.88724	1.00000				
7	.63949	.56953	.23136	.61876	.61091	.62450	1.00000			
8	.97825	.94604	.51530	.92705	.97758	.90841	.64993	1.00000		
9	.85967	.76233	.38210	.83057	.79568	.73829	.51616	.85152	1.00000	
10	.69227	.70604	.28047	.67550	.75603	.68944	.42239	.76881	.62551	1.00000

facies and which were not taken into account in the carbonate microfacies analysis (Table 2).

The ideal shallowing-upward sequence of the Joachim Dolomite with the vertical variation of the petrographic constituents and its general environmental evolution (Figures 3 and 4) is better described when it is transformed into a horizontal depositional model according to Walther's rule (Figures 5 and 6).

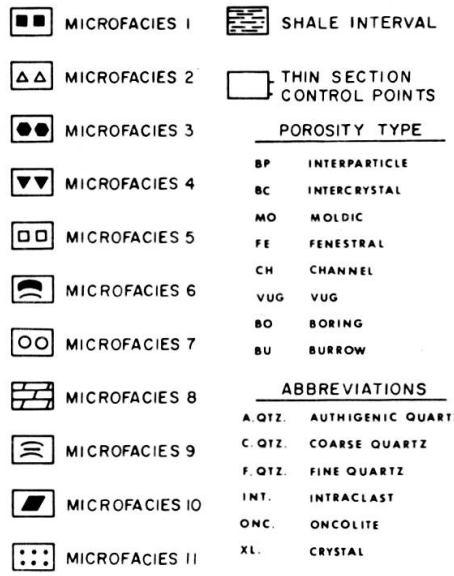

FIG. 3. — Table of symbols.

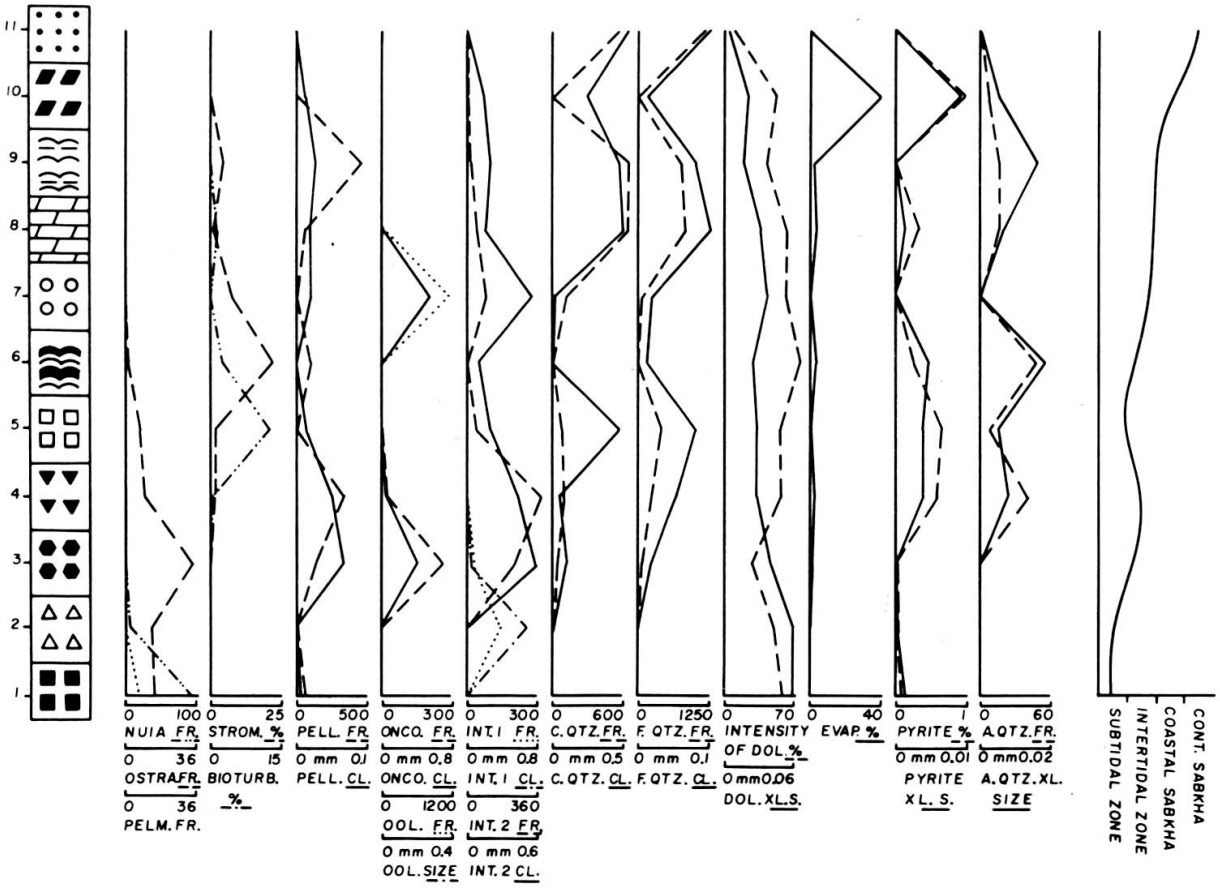

FIG. 4. — Ideal shallowing-upward sequence.

DESCRIPTION

The Joachim Dolomite was deposited in a generally shallow, low energy, restricted and hypersaline environment, periodically exposed, subjected to storms and invaded by dunes.

The horizontal juxtaposition of microfacies (Figures 5 and 6) has been interpreted geomorphologically in a landward direction as follows: offshore, shoreface, intra-bioclastic bar, back-bar flat, lagoon, stromatolitic ridge, oolitic flat, carbonate flat, inner stromatolitic ridge, evaporitic flat and dunes. In the same direction, the depositional environments are as follows: subtidal zone, intertidal zone, supratidal coastal sabkha and continental sabkha.

The variations of the averages for frequency, clasticity, and percent surface area for each component or non-particulate constituent (Tables 1 and 2) for the various microfacies are expressed by curves drawn below the graphic representation of the depositional model.

VARIATIONS OF COMPONENTS

The highest frequency of pelmatozoans occurs in offshore conditions (microfacies 1) indicating that their main habitat was located seaward. The frequency of pelmatozoans decreases rapidly landward because of increasingly unfavorable living conditions.

Nuia forms a dense population in offshore conditions (microfacies 1). Its behavior is similar to that of the pelmatozoans but is even more dispersed on the seaward side of the intra-bioclastic bar.

The ostracodes show their peak of frequency on the intra-bioclastic bar (microfacies 3). Apparently this is the result of a mechanical accumulation by passive flotation. The frequency decreases rapidly on both sides of the bar and then continues to decrease slowly landward. The gradual increase seaward indicates that the habitat of the ostracodes was located offshore.

Stromatolite mats reach their maximum development in the constructed stromatolitic ridge (microfacies 6). Their rapid seaward decrease correlates with the increase of the bioturbation intensity in the lagoon indicating that the lower limits of the algal mats were biologically controlled. The stromatolite mats decrease in frequency across the oolitic and carbonate flats (microfacies 7 and 8) and terminate with a small peak of frequency corresponding to the inner stromatolitic ridge (microfacies 9). This landward limit of the stromatolite mats coincides with the upper limit of the intertidal zone and was apparently controlled by desiccation.

Both the frequency and clasticity curves of the oncolites show their peaks in coincidence with the intra-bioclastic bar (microfacies 3) which offers the required conditions of agitation for their generation by destruction of stromatolitic mats.

Bioturbation is most extensive in the lagoon (microfacies 5) and shows a small peak in shoreface conditions (microfacies 2).

The frequency and clasticity of intraclasts 1 reach their peaks in shoreface (microfacies 2) and then decrease both seaward and landward. This indicates that their maximum production and accumulation in shoreface conditions probably resulted from some periodic strong currents.

The frequency of intraclasts 2 is high on the bar and reaches its peak in the back-bar flat (microfacies 4). The clasticity of intraclasts 2 does not coincide with the frequency peak, this indicates active production by periodic exposure of the bar (microfacies 3) and distribution behind it (microfacies 4). The clasticity curve has a second high peak in the oolitic flat because of a local relative increase in energy.

The frequency and clasticity curves of the lithic pellets are almost parallel to those of intraclasts 2 indicating that they originated from them. There is the same lack of coincidence between peaks with the highest clasticity on the bar (microfacies 3) and the highest frequency of distribution behind it (microfacies 4). The frequency curve shows a second peak in the inner stromatolitic ridge (microfacies 9), which indicates periodic exposure of that area as well.

The superficial ooids show peaks of their frequency and clasticity in coincidence with the oolitic flat (microfacies 7) where they were generated by moderate local agitation in a supersaturated environment. Their occurrence correlates with the second maximum peak of the clasticity of intraclasts 2 which confirms the local conditions of relatively higher energy, some superficial ooids having nuclei consisting of intraclasts 2.

The frequency and clasticity of the coarse quartz display their highest values in the dune environment (microfacies 11), and both decrease seaward with several fluctuations. This shows a continental source for the quartz with dispersion across the carbonate system. The frequency and clasticity curves are almost parallel with each other indicating a steady supply and distribution of the grains. The peaks which coincide with the carbonate flat (microfacies 8) and lagoon (microfacies 5) result from trapping effects of the eolian sand in depressions.

The frequency and clasticity of the fine quartz show their highest values in the dune environment (microfacies 11). They are perfectly parallel with each other and with the frequency and clasticity curves of the coarse quartz indicating similarity in transportation processes and depositional conditions.

Dolomitization is expressed by two curves: intensity in percent surface and crystallinity by means of the size of the rhombs. The curve of the intensity of dolomitization actually expresses the juxtaposition of two distinct processes. The first one involved the span of environments extending from offshore (microfacies 1) to lagoon (microfacies 5) and appears with a symmetrical intensity increasing on both sides of a low corresponding to the intra-bioclastic bar (microfacies 3). This situation is best explained by a model of freshwater-seawater mixing (Dorag model)

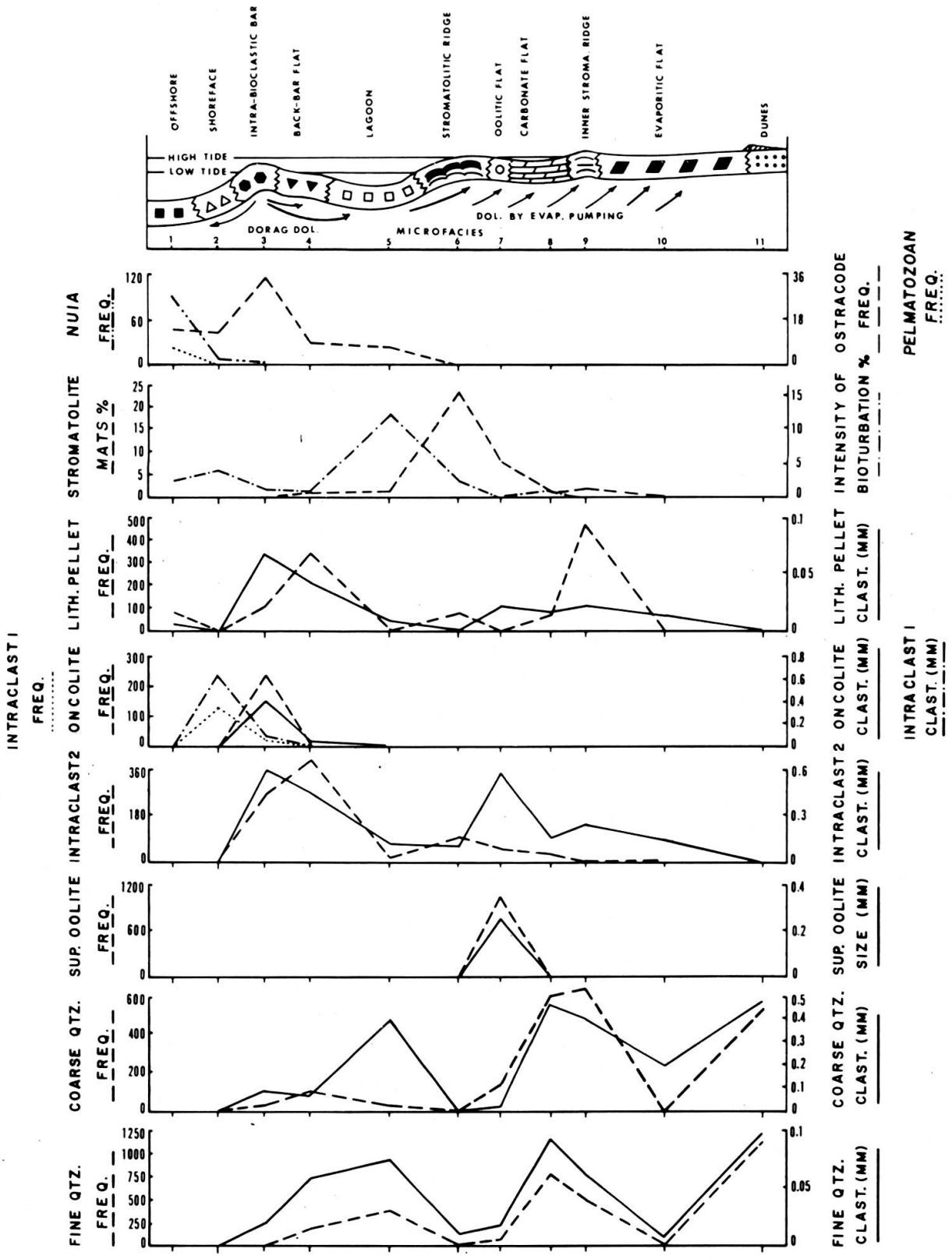

FIG. 5. — Horizontal environmental interpretation of microfacies.

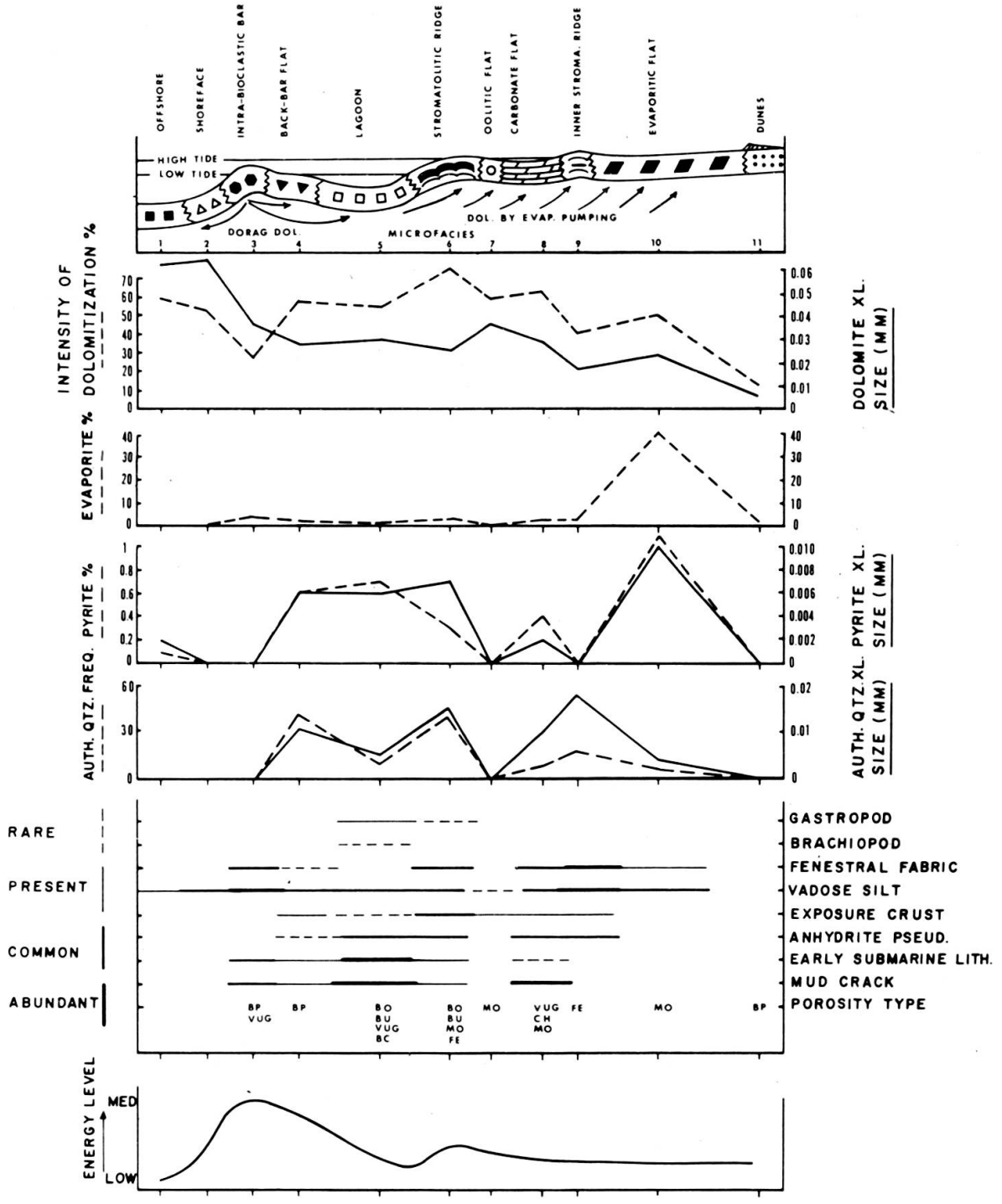

FIG. 6. — Horizontal environmental interpretation of microfacies.

generated by an active freshwater lens below the intra-bioclastic bar (Hanshaw, *et al.*, 1971; Badiozamani, 1973; Land, 1973a, b).

The second process involves the span of environments extending from the stromatolitic ridge (microfacies 6) to the evaporitic flat and the dunes (microfacies 10 to 11). It shows a peak of intensity of dolomitization in the stromatolitic ridge and a step-like decrease landward. The environmental conditions under which this dolomitization occurs, mostly a sabkha supported by stromatolitic margins, are in favor of a mechanism of evaporative pumping of the lagoonal waters already partially concentrated (Hsü and Siegenthaler, 1969; McKenzie *et al.*, 1980), a situation which explains the greater intensity of this process of dolomitization compared to the Dorag model.

It is quite possible that the decomposition of the organic matter of the stromatolites and the release of the magnesium they concentrate in their sheath material may contribute to the process of dolomitization (Gebelein and Hoffman, 1973; Davis and Ferguson, 1975; Mansfield, 1979).

The crystallinity of the dolomite expressed by the size of the rhombs shows a step-like increase oceanward across the entire carbonate system from microfacies 11 (eolian) to microfacies 2 (shoreface) followed by a slight decrease in microfacies 1 (offshore), as if it were independent of the two juxtaposed processes. In fact, the variation of size of the dolomite crystals is a generalized expression of the change of grain-size of the original carbonate being replaced, consequently the shape of the curve of crystallinity of the dolomite is parallel to that of the energy of the environment. This "blueprint" relationship between dolomite crystal-size and depositional grain-size has been observed previously in other carbonate environments (Zadnik and Carozzi, 1963).

The evaporite percent curve reaches its peak in the evaporitic flat (microfacies 10) where the highest rate of evaporation would be expected.

The pyrite percent and pyrite crystal size curves are almost parallel. They show their highest peaks in the evaporitic flat (microfacies 10) indicating that the pyrite crystals were formed as a result of subsurface sulfate reduction. The other smaller peaks in the carbonate flat (microfacies 8), during the span back-bar flat-lagoon-stromatolitic ridge (microfacies 4-5-8), and toward offshore (microfacies 1) appear related to reducing conditions due to local restriction or deepening of the environment of deposition.

The frequency and crystal size curves of authigenic quartz are parallel. Three peaks are apparent: back-bar flat (microfacies 4), stromatolitic ridge (microfacies 6) and inner stromatolitic ridge (microfacies 9). The only common character of these three environments is the abundance of organic matter which may have promoted this authigenesis.

Fenestral fabrics frequently occur in the intraclastic bar (microfacies 3), the stromatolitic ridge (microfacies 6), the oolitic flat (microfacies 7) through the inner

stromatolitic ridge (microfacies 9) indicating relatively high standing areas with periodic exposures and degassing of the sediments. Exposure crusts are mostly found in the stromatolitic ridge (microfacies 6) which also indicates high standing areas. Vadose silt is very widespread, it mostly coincides with fenestral fabrics and exposure crusts but has most probably been redistributed by vadose water circulation. Early marine lithification occurs from the bar (microfacies 3) into the lagoon (microfacies 5) and mud cracks are present mostly in the lagoon (microfacies 5) and the carbonate flat (microfacies 8); both features indicate temporary exposure associated with wetting and drying of the sediments. Anhydrite pseudomorphs occur throughout the coastal sabkha (microfacies 6-9) and into the lagoon (microfacies 5) due to local dissolution by circulating waters.

The relative energy of the environment is generally low with a minimum in offshore conditions. It increases up-slope, toward the intra-bioclastic bar where it reaches its peak. The energy curve shows a smaller increase in coincidence with the stromatolitic ridge (microfacies 6) and decreases gradually landward.

DIAGENESIS

Dolomitization and silicification

The most important diagenetic process affecting the Joachim Dolomite is naturally dolomitization. With respect to time relationships it has been shown for microfacies 1 through 5 that the main episode of dolomitization took place after the precipitation of a beachrock or submarine isopachous rim cement of aragonite or high-Mg calcite on the walls of interparticle pore spaces, and before the introduction of vadose silt and precipitation of freshwater vadose to phreatic poikilotopic calcite cement which obliterated all remaining porosity (Plate 1, E and Plate 2, A). The features of this dolomitization fit quite well with a freshwater-seawater mixing process which has affected completely the isopachous rim cement perhaps, because it consisted of high-Mg calcite, and partially to completely the micrite matrix, the intraclasts and the bioclasts (Plate 1, B). No time relationship of dolomitization with the original carbonate has been found for microfacies 6 to 11. Dolomitization is attributed here to a process of evaporative pumping in a sabkha environment and its relations to primary sedimentary structures and environmental setting confirm a subcontemporaneous to very early diagenetic replacement.

The time relationship between dolomitization and silicification is shown by the partial replacement of euhedral crystals of authigenic quartz by dolomite rhombs. Hence silicification preceded dolomitization.

The only exception to the above mentioned general interpretation of dolomitization as an early diagenetic process consists of floating dolomite rhombs

occurring in the cavity filling sparite of microfacies 8. Freeman (1966b) found also some dolomite rhombs floating within pore filling calcite cement in the Joachim strata of northern Arkansas, and concluded that dolomite was as late as this calcite cement, if not later. This feature obviously corresponds to late diagenetic dolomite related to burial subsurface processes (Mattes and Mountjoy, 1980).

Cementation

Isopachous rim cement is developed around carbonate grains and also on the walls of vugs and borings. It has been interpreted as representing submarine or beachrock cementation consisting of either aragonite or high-magnesium calcite. It was subsequently dolomitized and in most cases overlain by poikilotopic or blocky sparite cement which filled most of the remaining cavities.

Poikilotopic sparite is the most important cement occurring in the Joachim Dolomite and essentially obliterates porosity. It filled interparticle pores, vugs, borings, cracks of desiccation breccias, and fenestral pore spaces. It has also replaced mosaic and crystalline anhydrite. This cement is late diagenetic and in most cases associated with vadose silt. It has been interpreted as precipitated from freshwater in the vadose or phreatic zone.

Blocky sparite is found in microfacies 1, 2, 3 and 5 but in small amount compared to the poikilotopic sparite cement with which it shares the same origin.

Authigenic quartz

The crystals of authigenic quartz appear with hexagonal and diamond shapes in thin section (Plate 3, H). They are best developed within the cavities of dissolved anhydrite. It seems that the diamond shape quartz individuals are pseudomorphs after anhydrite crystals whether or not they are doubly terminated. As mentioned above the authigenic quartz crystals are partially replaced both by dolomite rhombs, and by void filling poikilotopic sparite cement (Plate 3, H). This indicates that they represent the earliest diagenetic process of the carbonate system.

Authigenic K-feldspar

Euhedral crystals of authigenic K-feldspar are found only in core samples. They are randomly oriented with lengths of 0.2 to 0.4 mm. The common association of alkaline minerals and authigenic feldspar with hypersaline, alkaline brines has been noted by Jones (1961), Hay and Moiola (1964), and Füchtbauer (1972). Mazzullo (1976) reported the overgrowths of authigenic K-feldspar on detrital nuclei, as well as single crystals of similar mineralogy in Cambro-Ordovivian carbonate rocks of the Proto-Atlantic shelf in North America from sabkha deposits. He con-

cluded that authigenic feldspar growth occurred in a chemical system that allowed crystallization to proceed under optimal conditions of high activity ratio of K^+/H^+ in brines saturated with silica.

Evaporite diagenesis

The most important diagenetic process affecting evaporites is dissolution which is shown by preserved crystal moldic porosity, calcite pseudomorphs after anhydrite and gypsum, collapse breccias, and smaller volume of preserved evaporites in outcrop samples in comparison with larger amounts of preserved evaporites in core samples of similar microfacies.

Anhydrite and gypsum crystals of the outcrop samples were dissolved and refilled by poikilotopic sparite cement, or totally dissolved leaving crystal moldic porosity with a few exceptions in which crystals of gypsum were preserved. Calcite pseudomorphs after anhydrite display crystalline and nodular mosaic structures (Plate 3, D). In core samples the dominant evaporitic mineral is anhydrite. Gypsum is found only as a weathering product of anhydrite filling fractures and cracks. This is to be expected since gypsum does not occur at depths greater than 500 m in the subsurface.

Displacement, dissolution, and reprecipitation are important diagenetic changes of anhydrite in core samples. Anhydrite displacement initiates the formation of diapiric structures, or brecciation. The cracks of the brecciated samples are filled by anhydrite cement.

The individual crystals and nodules of anhydrite found in core samples display the typical and well-known features of the near-surface generation of anhydrite in coastal sabkha environment.

Several specimens with molds of hopper and of simple cubic-shaped halite have been found in outcrop samples. In all instances these molds were completely empty corresponding to crystal-moldic porosity. Halite hoppers have been reported by Handford and Moore (1976) from the Joachim Dolomite of northern Arkansas which were filled by two generations of calcite cement, a thin rim cement (subsequently dolomitized) and cavity filling sparite cement. They concluded that the halite grew within the sediments from upward moving phreatic marine waters by an evaporative pumping mechanism which dolomitized the tidal flat sediments. This episode was followed by tidal flat progradation and influx of mixed meteoric-marine water which dissolved the halite, precipitated the calcite rim cement, and converted it to dolomite. In the final stage, meteoric water completely dominated the subsequent diagenesis which resulted in precipitation of calcite cement and obliteration of the remaining porosity. This model is not fully applicable to the hoppers found in this study, since they are not filled by any cement. It seems that the halite of the investigated area was formed by the evaporative pumping mech-

anism responsible for the dolomitization of the coastal to continental sabkha dune environment (stromatolitic ridge through dune), and simply dissolved out later as a result of weathering.

Collapse breccias with a typical puzzle-like appearance consisting of clasts of micrite with an interstitial cement of poikilotopic calcite (Plate 2, H) are frequently found in the Joachim Dolomite. They result from one or several episodes of subsurface dissolution of intercalated halite by groundwaters.

COMPARISON WITH RECENT AND ANCIENT ANALOGUES

The reconstruction of the depositional model of the Joachim Dolomite has been based on the concept that it was an Ordovician analogue of the Recent sabkha sediments along the Trucial Coast of the Persian Gulf. The latter display a regressive vertical succession from lagoonal conditions through intertidal algal mats into a supratidal flat environment with its typical assemblage of diagenetic sulfate minerals, which was designated by Shearman (1966) as the *sabkha cycle* of sedimentation and early diagenesis.

Upon comparing the various facies of the sabkha environment of the Trucial Coast and their cyclic evolution with the microfacies of the Joachim Dolomite and their shallowing upward sequence (Figure 4), the similarities of depositional and diagenetic features are sufficiently striking at all levels of observation to justify the interpretation of the Joachim Dolomite as a Middle Ordovician coastal to continental sabkha (Figures 5 and 6). Naturally, the identity extends to other paleosabkhas among which the Cambrian-Ordovician carbonates of northeastern North America and Queensland, Australia (Rubin and Friedman, 1977; Mazzullo and Friedman, 1977; Friedman and Radke, 1979); the Jurassic carbonate-evaporite sequence of the Arab Darb Formation off the Trucial Coast of Arabia (Wood and Wolfe, 1969); and the Jurassic carbonate sequence of the Aquitaine Basin (Bouroullec and Deloffre, 1982).

ENVIRONMENTAL SIGNIFICANCE OF THE UNIMODAL AND BIMODAL QUARTZ ARENITES

Layers of bimodal quartz arenite occur at different levels of the Joachim Dolomite (Augusta, Boles and Defiance Members). Their independent environmental characterization as eolian desert sands as well as a comparison with the Recent would be an additional important argument in favor of their interpretation as part of a continental sabkha. Statistical analyses were performed to test the bimodality of these grains using the SOUPAC statistical package. Samples with

TABLE 4

Grain Size Analysis of the Bimodal Arenites

Sample	Pair no.	No. of sample	Section	Mean	Difference	Paired std. error	DF	T	Prob.
Fine quartz	1	320	B	.1129000	.3545062	.6774487E-02	319.	52.32961	.00000
Coarse quartz	1	320	B	.4674062					
Fine quartz	2	220	E	.9075909E-01	-4332591	.7013135E-02	219.	61.77823	.00000
Coarse quartz	2	220	E	.5240182					
Fine quartz	3	190	F	.7852632E-01	.3700000	.5821058E-02	189.	63.56233	.00000
Coarse quartz	3	190	F	.4485263					
Fine quartz	4	50	J	.7960000E-01	-2910000	-1096655E-01	49.	26.53523	.00000
Coarse quartz	4	50.	J	.3706000					

Fine quartz grand mean: 0.096
Coarse quartz grand mean: 0.473

equal size of coarse and fine quartz grains were chosen and their clasticity index measured. Since the samples are identical in size, paired t comparisons were used to analyze the bimodal quartz grains using the following formula:

$$t_s = \frac{\bar{D} - (\mu_1 - \mu_2)}{S_{\bar{D}}}$$

where $\bar{D}$ is the mean difference between the paired observation, μ_1 and μ_2 are means of coarse and fine quartz, and $S_{\bar{D}}$ is the standard error of $\bar{D}$ calculated from the observed differences. The results of this analysis (Table 4, Figure 7) show that the

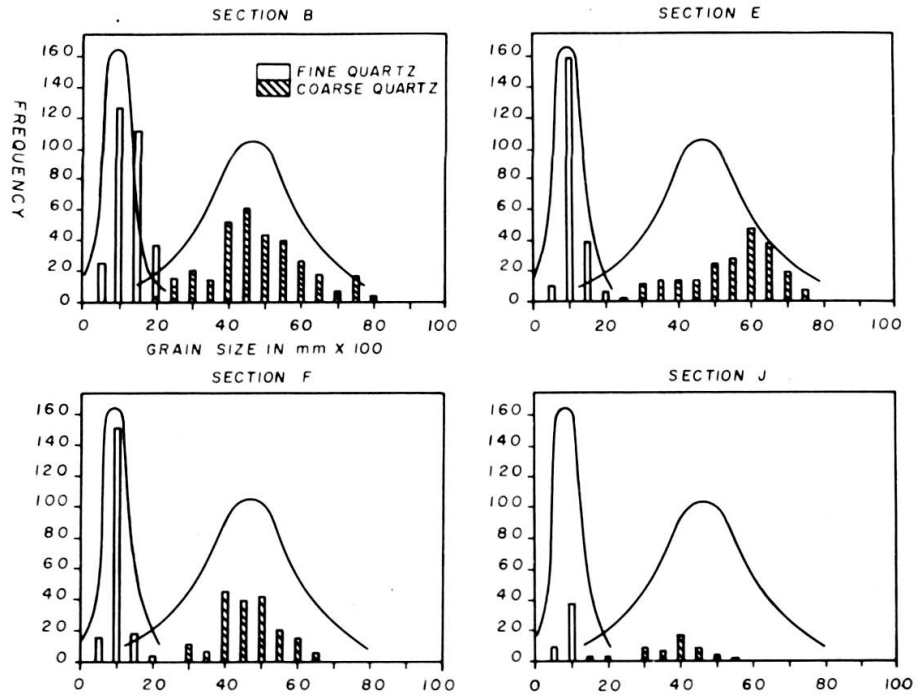

FIG. 7. — Histograms and corresponding theoretical curves showing distribution of bimodal arenites in sections B, E, F, and J.

calculated t is greater than its value in t-table, therefore, there is a detectable significance difference between population means of the fine and coarse quartz grains, and consequently the quartz arenite of the investigated sections are bimodal.

Udden (1898, in Folk, 1968) was the first to point out the occurrence of bimodal sand in desert lag deposits. He observed that the great majority of dune sand fell in the 0.125-0.25 mm size grade (fine sand). He stated that wind definitely selects sand of that size for dunes, regardless of location. Therefore it is a property of the eolian medium of deposition and not of any source terrane. Bimodal sands occur in interdune areas of the Algerian Sahara, the Libyan Sahara, the Simpson desert

of Australia, and many other places. Folk (1968) concluded that the two grain sizes are characteristic of modern desert lag sediments worldwide. He found the same bimodality in compositionally different sands and concluded that size distribution was not caused by any one particular source; rather it was the dynamic result of the process of eolian erosion and deposition. The main factor responsible for desert bimodality is the selective removal of the fraction that travels largely by saltation and its accumulation as dunes with a grain size of about 0.18-0.25 mm. Thus the desert floor becomes impoverished in this size grade, and relatively enriched in grains that can easily be rolled by the wind but are too large to saltate, and those that, if undisturbed and on a flat surface, are too small to be easily moved by the wind since they have a cohesive smooth surface; but once disturbed, they travel great distance in suspension (dust storms).

Bagnold (1941, in Folk, 1968 and Glennie, 1970) found out that for any given size of grain, there is a certain velocity of wind ("threshold velocity") at which the grains are set in motion. He showed that particles below 0.08 mm have a higher threshold velocity than larger particles: below this limit, the finer the grain size, the greater the threshold velocity, so that a wind which is strong enough to move grains 4.6 mm in diameter is unable to move finely scattered dust. This situation is accounted for by the existence of a wind velocity gradient of nearly zero close to the ground, therefore once fine solid particles smaller than about 0.03 mm have settled on the ground, they are left almost immobile by any ordinary wind.

From the previous observations, Folk (1968) concluded that ancient quartz arenites regardless of age or location, which display the above mentioned bimodality and grain size range should be interpreted as eolian desert sands. Therefore we may conclude that the unimodal (Plate 3, G) and bimodal quartz arenites (Plate 3, F) of the Joachim Dolomite were deposited under continental desert conditions respectively in dune and interdune areas. Moreover, the mixed carbonate-clastic sediments are interpreted as representing the progradation of dunes onto the carbonate-evaporitic shelf by strong winds blowing from land to offshore.

STRATIGRAPHIC SECTIONS AND VERTICAL SUCCESSION OF MICROFACIES

Two composite stratigraphic sections and one core cut through the entire formation were used to reconstruct three complete sections of the Joachim Dolomite in three localities in order to analyze the detailed vertical and horizontal variations of the depositional environments. The first composite section (Figures 8 to 11) consists of field sections A, B, C, D, and G which correspond to the type sections of the members as described by Templeton and Willman (1963). The second composite section consists of sections F and H and is not illustrated here, the lithologies

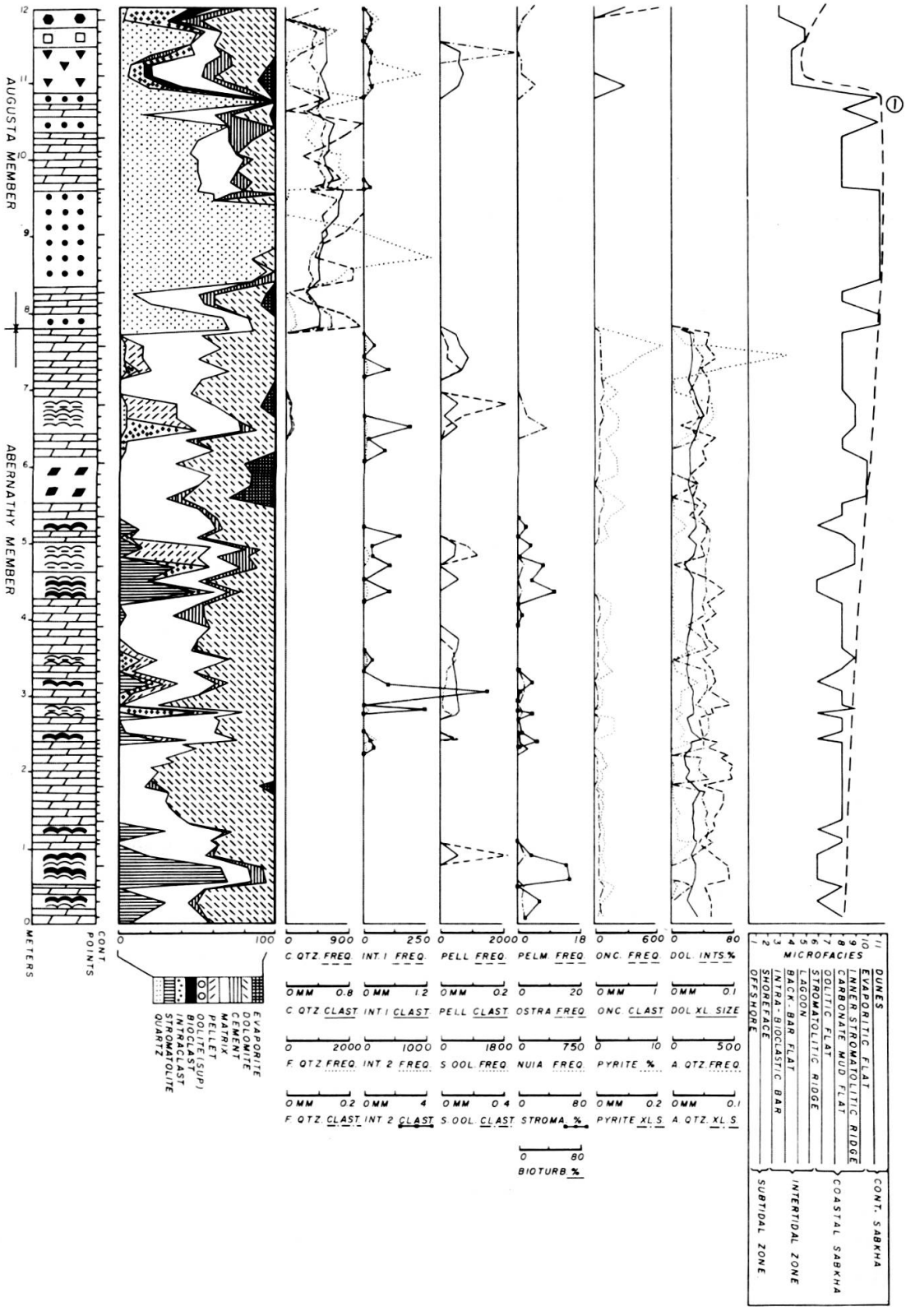

FIG. 8. — Components variations of the Joachim Dolomite: Section A (0.0 to 7.8 m), Section B (7.8 to 12.0 m).

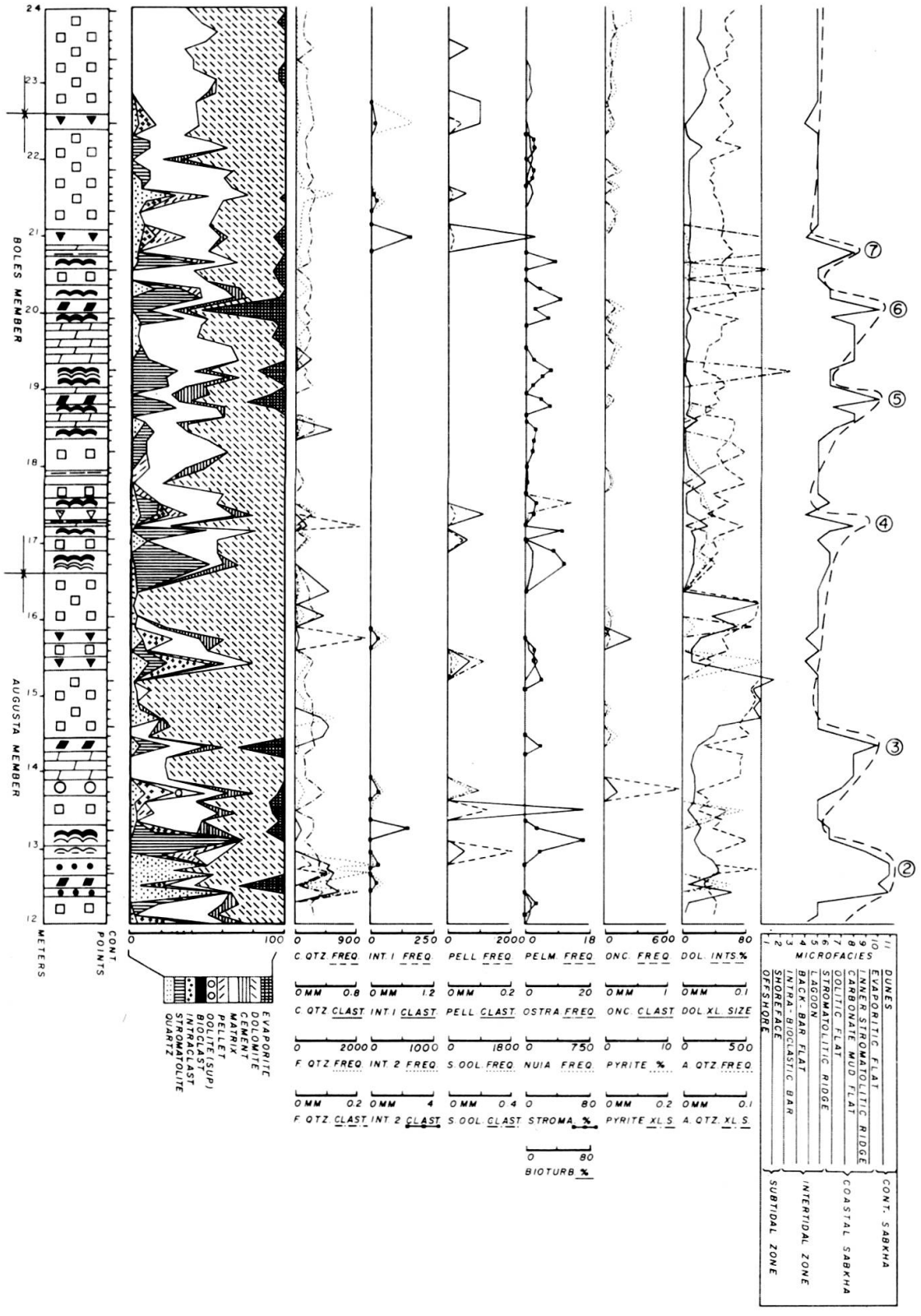

FIG. 9. — Components variations of the Joachim Dolomite: Section B (12.0 to 16.6 m), Section C (16.6 to 24.0 m).

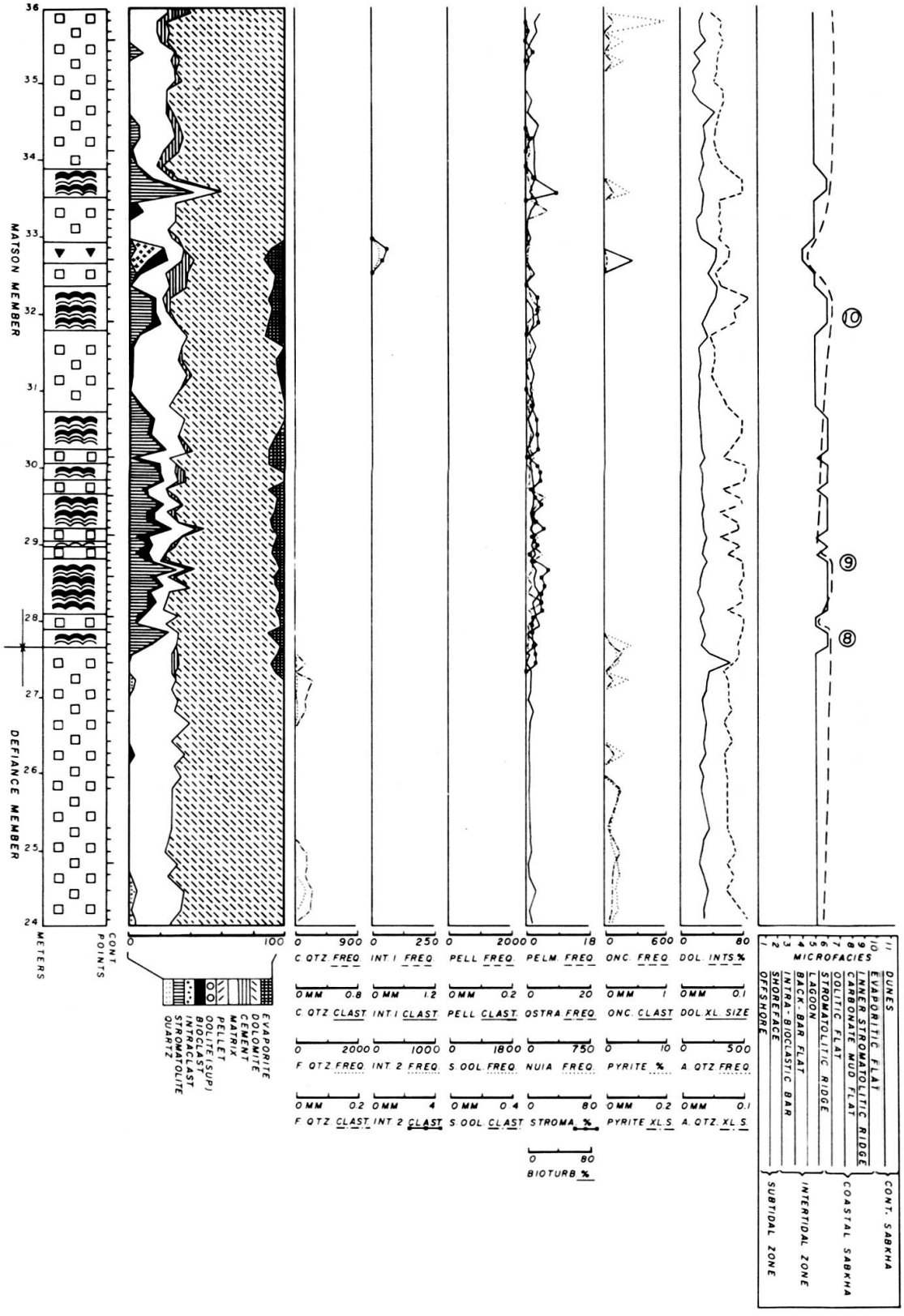

FIG. 10 — Components variations of the Joachim Dolomite: Section C (24.0 to 27.6 m), Section D (27.6 to 36.0 m).

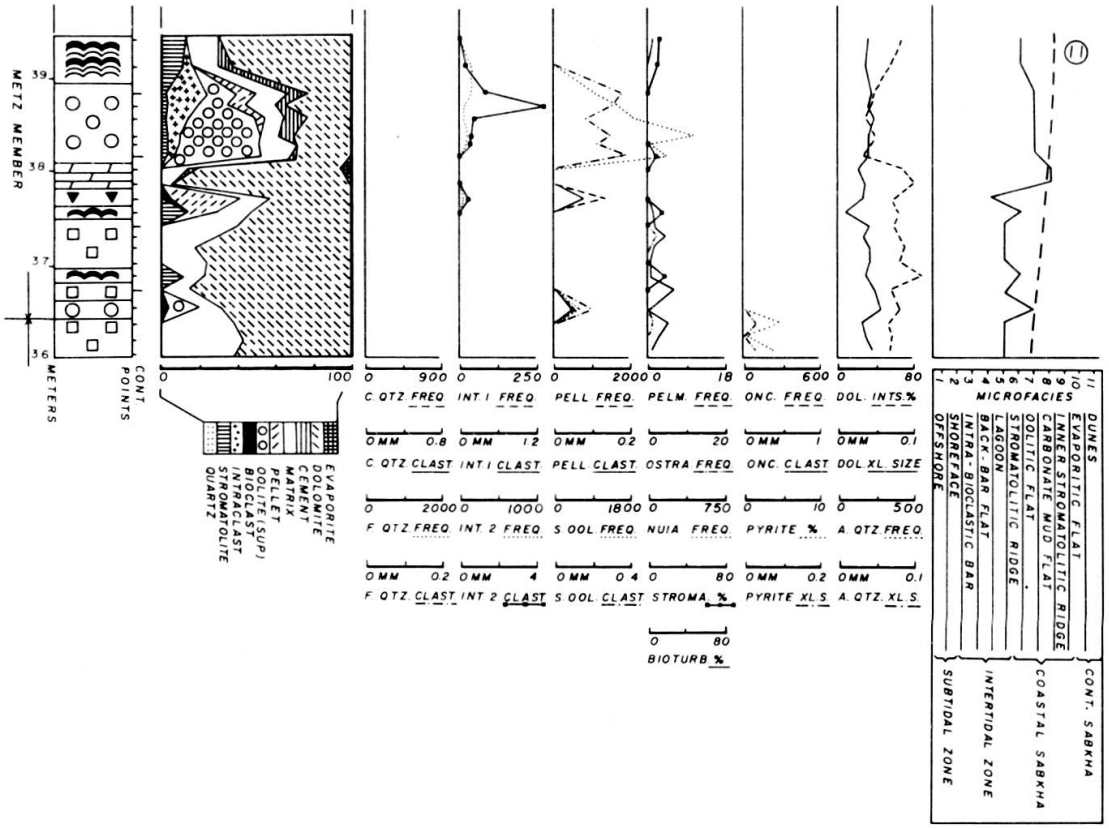

FIG. 11. — Components variations of the Joachim Dolomite: Section D (36.0 to 36.4 m), Section G (36.4 to 39.4 m).

being rather similar to those of the first composite section (see Okhravi, 1982). The core has been designated as section K (Figures 12 and 13). It represents an environment richer in evaporites than the two other composite sections and a subdivision into members could be attempted only by means of microfacies data. Therefore, the subdivisions of section K are designated as "equivalent evaporitic members" pending their subsequent naming on a lithostratigraphic basis.

The graphic representation of the investigated sections is using the following modes of expression from left to right:

1. Column of microfacies with metric scale and control points.
2. Graphic log representing the variations of the major mineralogical and textural components in percent surface area.
3. Sets of variation curves of the clasticity and frequency of the major depositional and diagenetic constituents.
4. An environmental curve (Carozzi and Diaby, 1982), which has a scale corresponding to the depositional model (solid line). Cycles are designated by

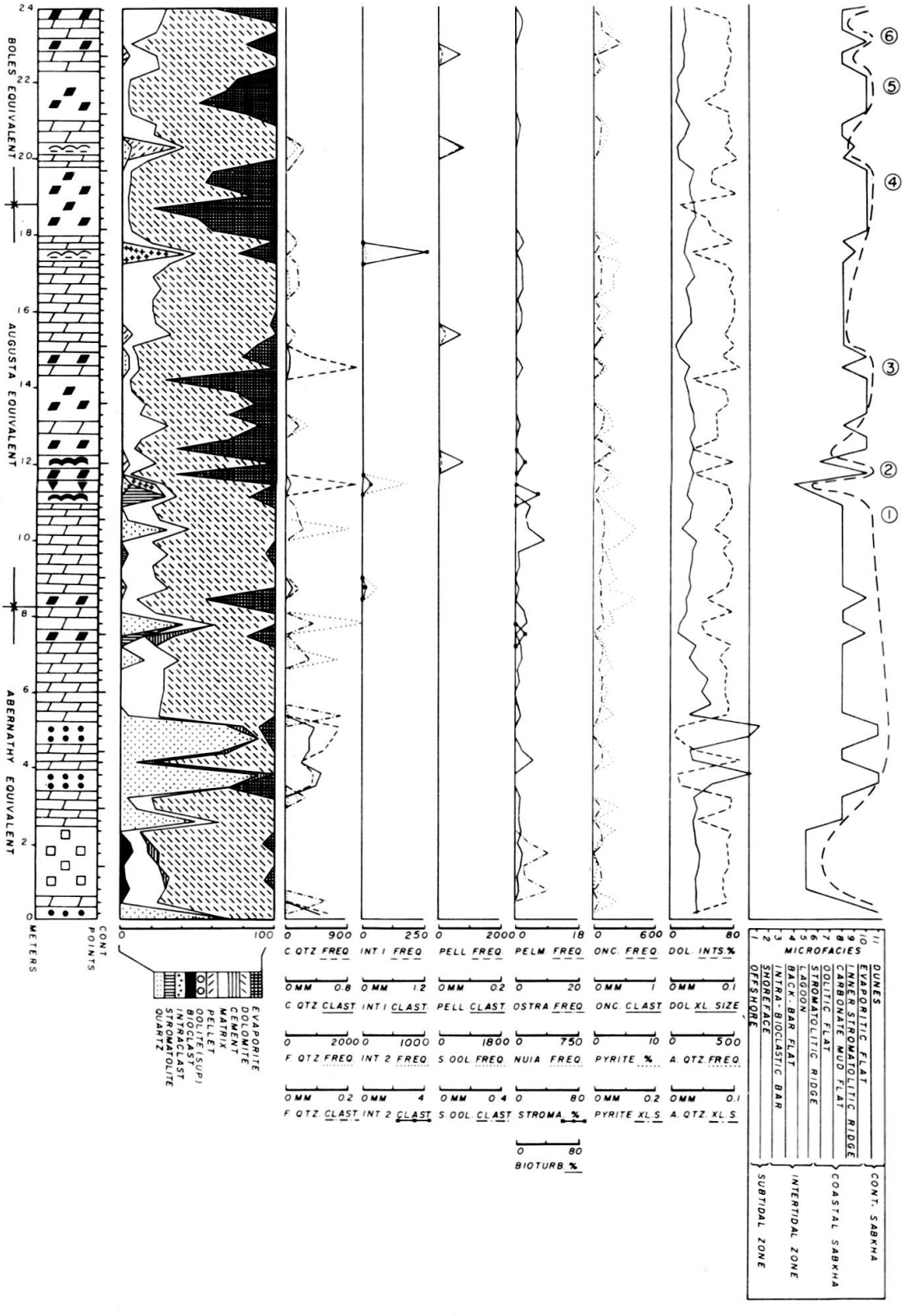

FIG. 12. — Components variations of the Joachim Dolomite: Section K (0.0 to 24.0 m).

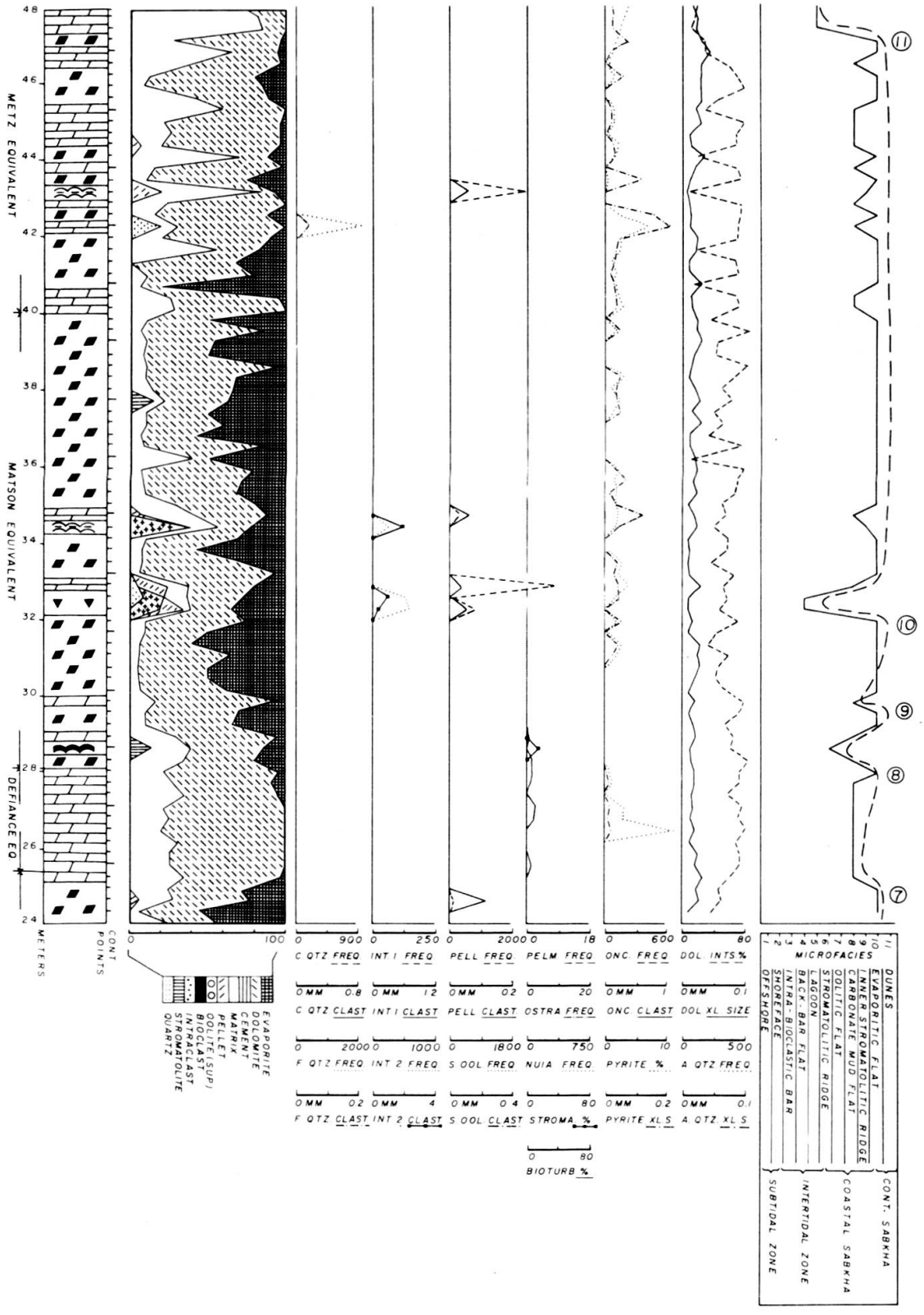

FIG. 13. — Components variations of the Joachim Dolomite: Section K (24.0 to 48.0 m).

circled Arabic numerals. The asymmetric cycles consist of a slow shallowing-upward phase followed by a rapid deepening phase, the typical trademark of carbonate deposition. The large-scale evolution of the environments which also consists predominantly of asymmetric megacycles is indicated by a tangential dashed line.

There is a general lack of agreement between the boundaries of the six members defined by Templeton and Willman (1963) on the basis of megascopic field criteria such as types of bedding and relative sand, silt and shale content, and the subdivisions corresponding to the small-scale asymmetric cycles and large-scale asymmetric megacycles obtained by means of the microfacies approach and the petrographic measurements. This is to be expected since the two approaches operate at two entirely different scales, but it is obvious that the field lithostratigraphic units represent the indispensable basis for the subsequent petrographic refinements.

The graphic representation is self-explanatory and does not require any additional comments. The data presented here were used as a basis for the preparation of the depositional-diagenetic model.

GENERAL EVOLUTION OF DEPOSITIONAL ENVIRONMENTS

The environmental curves of the two composite sections and of the core (Figures 14 to 16) indicate that each section consists of the superposition of eleven asymmetric depositional cycles. Further analysis shows that it is possible to associate these cycles into four large-scale distinct episodes (designated by Roman numerals) which either correspond to asymmetric megacycles or to intervals of time during which the small-scale asymmetric cycles present strong similarities in size, amplitude or pattern.

Episode I

In the first composite section (Figure 14) this episode corresponds to a single asymmetric megacycle which starts in the carbonate flat (microfacies 8) and terminates in the coastal sabkha or the dunes (microfacies 10-11). This episode in the second composite section (Figure 15) begins in the relatively deeper condition of the intra-bioclastic bar (microfacies 3) and terminates at the inner stromatolitic ridge (microfacies 9). In section K (Figure 16) this episode begins at the stromatolitic ridge (microfacies 6) and stays for a very long period of time in the evaporitic flat (microfacies 10) and terminates in it.

In summary, composite section No. 2 representents relatively deeper environments than composite section No. 1, whereas section K shows the shallowest conditions.

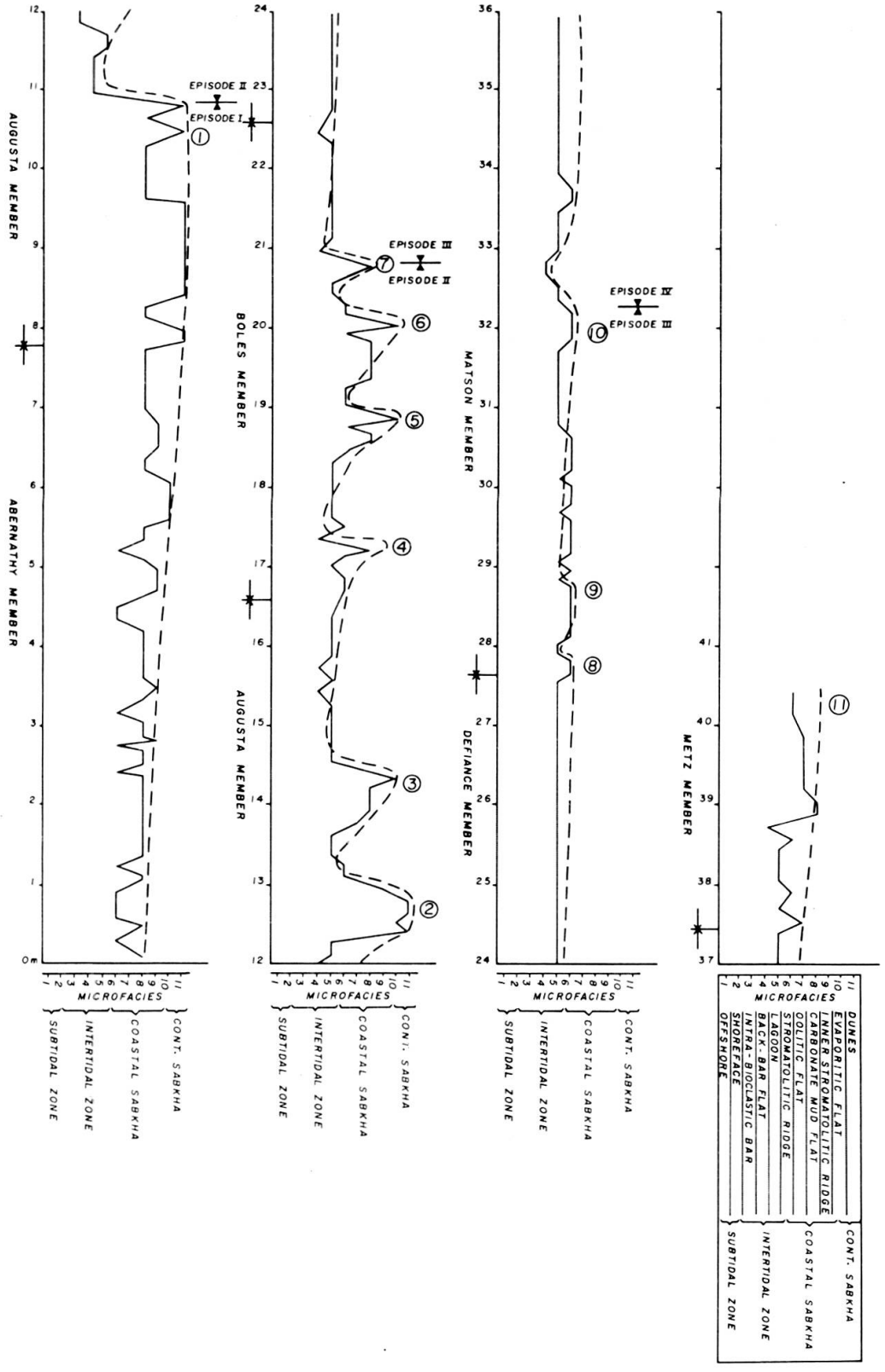

FIG. 14. — Environmental evolution and cyclicity of the Joachim Dolomite (Sections A, B, C, D, and G).

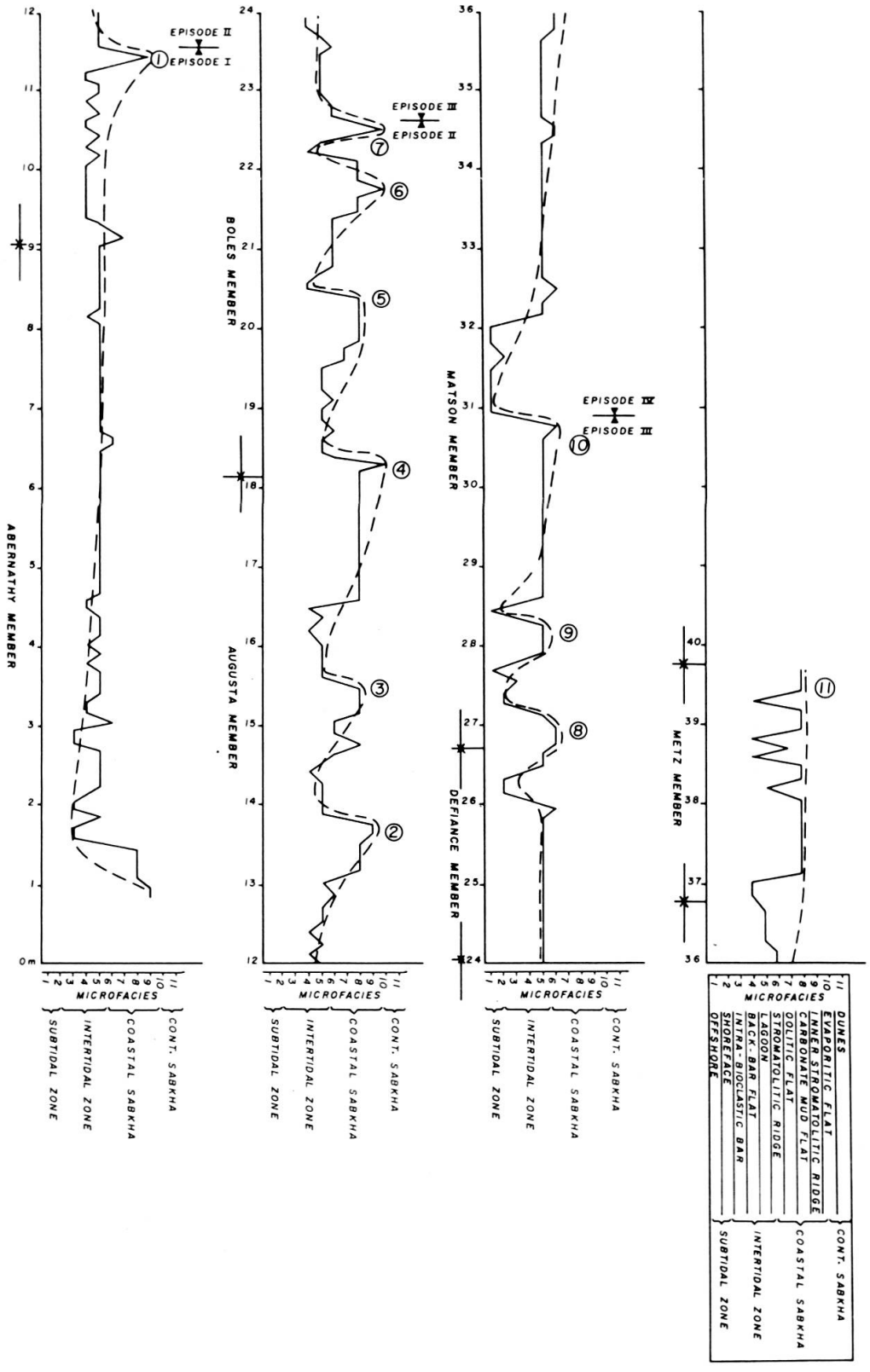

FIG. 15. — Environmental evolution and cyclicity of the Joachim Dolomite (Sections F and H).

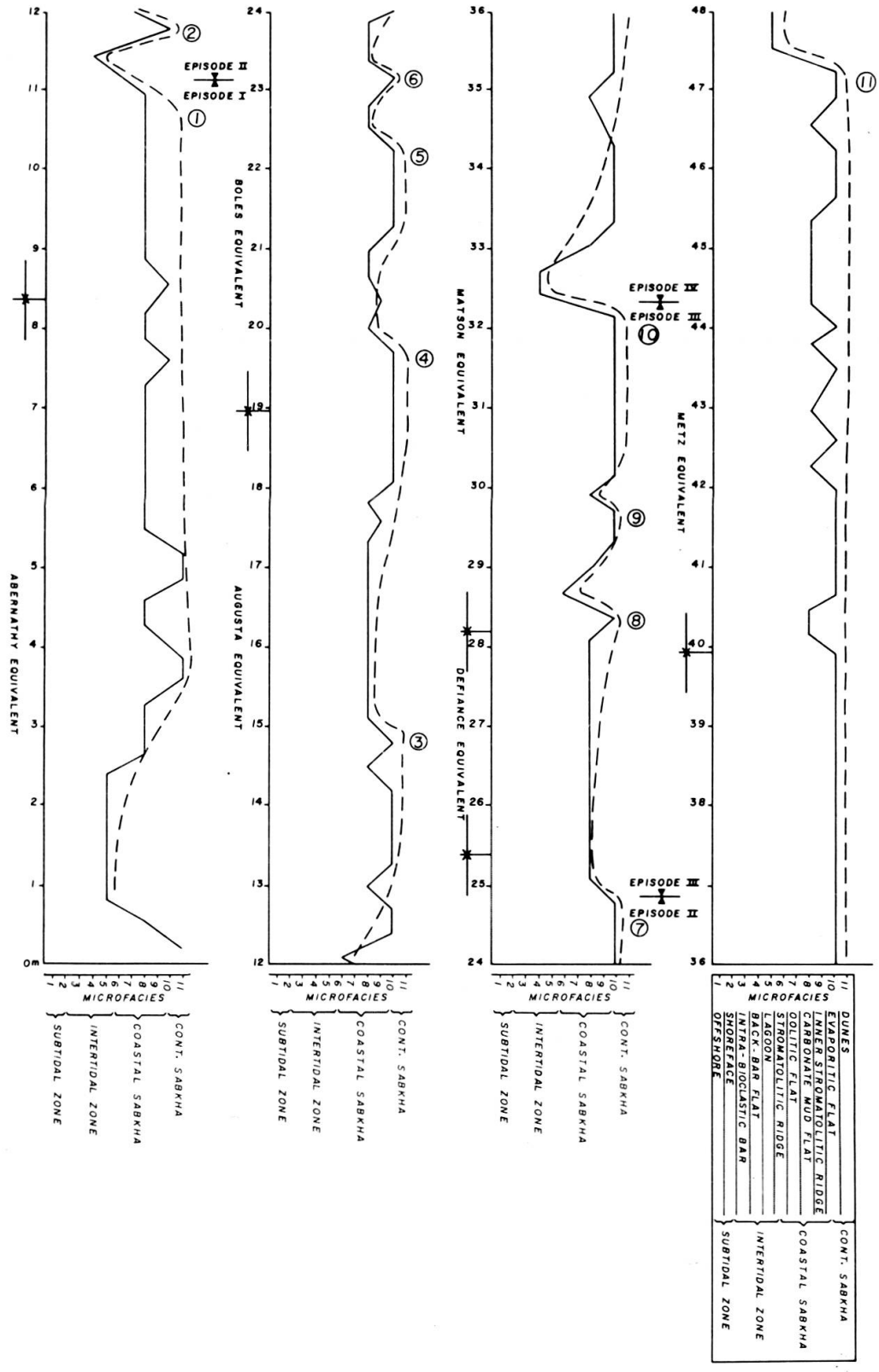

FIG. 16. — Environmental evolution and cyclicity of the Joachim Dolomite (Section K).

EPISODE II

In the first composite section (Figure 14) this episode is characterized by a general deepening of the environment and oscillations which are expressed by the succession of six small-scale asymmetric cycles which usually begin at the intra-bioclastic bar (microfacies 3) or the back-bar flat (microfacies 4) and generally terminate in the evaporitic flat (microfacies 10) or the dunes of the continental sabkha (microfacies 11). In composite section No. 2 (Figure 15) the picture is almost identical with termination of the small-scale asymmetric cycles mostly between the carbonate flat (microfacies 8) and the evaporitic flat (microfacies 10). In section K (Figure 16) the pattern of the six small-scale asymmetric cycles begins at the back-bar flat (microfacies 4), but most of the cycles start at the carbonate flat (microfacies 8) and terminate at the evaporitic flat (microfacies 10).

In summary, again composite section No. 2 oscillates in slightly deeper conditions than composite section No. 1, whereas section K shows again the shallowest conditions.

EPISODE III

In the first composite section (Figure 14) this episode is characterized by a continuation of the general deepening of the environment. It consists of three small-scale asymmetric cycles which begin at the lagoon (microfacies 5) and terminate at the stromatolitic ridge (microfacies 6). In composite section No. 2 (Figure 15) this episode also shows three small-scale asymmetric cycles which generally begin in the offshore (microfacies 1) and terminate at the stromatolitic ridge (microfacies 6). In section K (Figure 16) the same three small-scale asymmetric cycles begin at the stromatolitic ridge (microfacies 6) or the carbonate flat (microfacies 8 and terminate at the evaporitic flat (microfacies 10).

In summary, for the third time composite section No. 2 is in relatively deeper conditions than composite section No. 1 and section K is in the shallowest conditions.

EPISODE IV

In the first composite section (Figure 14) this episode corresponds to a single large-scale asymmetric megacycle which begins at the back-bar flat (microfacies 4) and terminates at the carbonate flat (microfacies 8). In composite section No. 2 (Figure 15) the same megacycle begins in deeper conditions in offshore (microfacies 1) and terminates at the carbonate flat (microfacies 8). In section K (Figure 16) the megacycle of this episode begins at the backbar flat (microfacies 4) and terminates at the evaporitic flat (microfacies 10).

In summary, for the fourth time composite section No. 2 is in relatively deeper conditions than composite section No. 1 and section K is in the shallowest con-

ditions. These constant differences of the environmental evolution represent the effect of paleogeographic conditions that cannot be fully evaluated at this time because of the lack of knowledge of the entire carbonate basin in which the Joachim Dolomite was deposited.

PALEOGEOGRAPHY

During the Middle Ordovician, the investigated area (Figure 17), was located at approximately 20°S (Ziegler *et al.*, 1979; Scotese *et al.*, 1979).

The prevailing winds were southeast trade (equal to east-west direction of present time), but some short-lived periodic winds blowing from the northeast

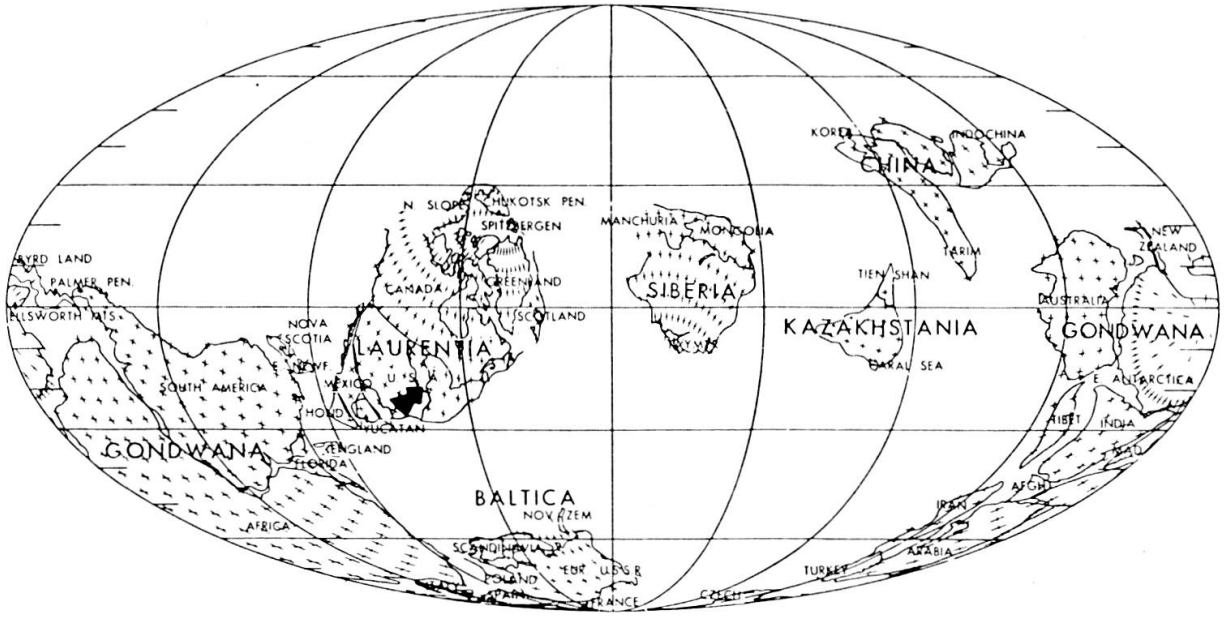

FIG. 17. — Middle Ordovician (Llandeilian-earliest Caradocian) paleogeography. Mollweide projection "front view" (an equal area view of the entire surface of the earth). The parallels of latitude are spaced 10 degree apart along the margins of the map and drawn completely at 30 degree intervals (after Scotese *et al.*, 1979). The investigated area is shown by an arrow.

(equal to north-south direction of present time) were responsible for the invasion of the carbonate platform by desert dunes. These dunes were formed by pure quartz sand derived from St. Peter "sands" mostly exposed during the time of deposition of the lower portion of the Joachim Dolomite and dispersed southward on the Joachim sabkha. This belt of pure quartz sand has been interpreted as a system of barrier islands forming the southern limit of a shallow basin with tidal flats located in northern Illinois and southern Wisconsin (Fraser, 1976).

The core (section K) located approximately 100 miles eastward of the outcrop belt displays even more accentuated sabkha features, for instance, a greater amount of evaporites. This situation indicates an extremely widespread and flat sabkha environment which might have extended at least as far as the Illinois-Indiana border, with an open sea direction toward the south.

CONCLUSIONS

This petrographic-microfacies study of the Joachim Dolomite led to the identification of 11 distinct carbonate-evaporite and clastic microfacies. The study of the detailed stratigraphic superposition and bivariate correlation analysis of the various microfacies showed that they build an ideal shallowing-upward sequence which has been converted into a horizontal depositional model. Within the latter the different microfacies have been interpreted geomorphologically in a landward direction as expressing the following environments: offshore, shoreface, intrabioclastic bar, back-bar flat, lagoon, stromatolitic ridge, oolitic flat, carbonate flat, inner stromatolitic ridge, evaporitic flat and dunes. This succession of environments spans from the subtidal zone, through the intertidal zone, the supratidal coastal sabkha, and terminates with the continental sabkha and desert.

Unimodal and bimodal quartz arenites of the Joachim Dolomite deposited in respectively dune and interdune positions by winds were taken as an independent evidence to demonstrate the desert environment and its temporary extension over the carbonate system.

The offshore through lagoonal microfacies of the Joachim Dolomite were secondarily dolomitized by a freshwater-seawater mixing process (Dorag model), while the rest of the microfacies were dolomitized by an evaporitic pumping mechanism of sabkha type.

The general environmental evolution of the microfacies shows that a complete section of the Joachim Dolomite consists of the superposition of 11 asymmetric cycles which display a slow shallowing-upward phase followed by a rapid deepening phase, a typical feature of carbonate sedimentation. These small cycles are in turn associated into four episodes which can be either large-scale asymmetric megacycles or intervals of small asymmetric cycles which present strong similarities in size, amplitude or pattern.

Paleoclimatic data confirm that the investigated area was located during the middle Ordovician at the appropriate latitude for development of an arid climate and that the Joachim Dolomite can be interpreted as a large-scale sabkha covering the middle part of Illinois with a transition to open sea conditions in a southward direction.

LIST OF REFERENCES

BADIOZAMANI, K. (1973). The Dorag dolomitization model — application to the Middle Ordovician of Wisconsin: *Jour. Sed. Petrology*, v. 43, pp. 965-984.

BOUROULLEC, J. et R. DELOFFRE (1982). Les paléosebkhas du Jurassique terminal en Aquitaine: *Bull. Centres Rech. Explor.-Prod. Elf-Aquitaine*, v. 6, pp. 227-255.

CAROZZI, A. V. (1958). Micro-mechanisms of sedimentation in the epicontinental environment: *Jour. Sed. Petrology*, v. 28, pp. 133-150.

—— (1961). Reef petrography in the Beaverhill Lake Formation, Upper Devonian, Swan Hills area, Alberta, Canada: *Jour. Sed. Petrology*, v. 31, pp. 497-513.

—— A. V. and I. DIABY (1982). Microfacies of the Salem Limestone (Middle Mississippian), southwestern Illinois, U.S.A.: *VIII Congreso Geologico Argentino, San Luis, Actas*, v. II, pp. 435-457.

CHOQUETTE, P. W. and L. C. PRAY (1970). Geological nomenclature and classification of porosity in sedimentary carbonates: *Am. Assoc. Petroleum Geologists Bull.*, v. 54, pp. 207-250.

DAVIS, P. J. and J. FERGUSON (1975). Dolomite and organic material: *Nature*, v. 255, pp. 472-473.

DEMIRMEN, F. (1969). Multivariate procedures and FORTRAN IV program for evaluation and improvement of classifications: *Kansas State Geol. Survey, Computer Contrib.* 31, 51 p.

DICKSON, J. A. D. (1980). Staining thin sections: Alizarin red S and potassium ferricyanade stain: Unpublished, 2 p.

FOLK, R. L. (1962). Spectral subdivision of limestone types: in *Classification of Carbonate Rocks* (W. E. Ham, ed.), Am. Assoc. Petroleum Geologists Mem. 1, pp. 62-84.

—— (1968). Bimodal supermature sandstones: product of the desert floor: *Report XXIII Internat. Geol. Congress, Czechoslovakia*, v. 8, pp. 9-32.

FRASER, G. S. (1976). Sedimentology of a Middle Ordovician quartz arenite-carbonate transition in the Upper Mississippi Valley: *Geol. Soc. America Bull.*, v. 86, pp. 833-845.

FREEMAN, T. (1965). Post-lithification dolomite in the Joachim and Plattin Formations (Ordovician), north Arkansas (abs): *Program 1965 Annual Meeting Geol. Soc. America*, p. 58.

—— (1966*a*). "Petrographic" unconformities in the Ordovician of northern Arkansas: *Oklahoma Geological Notes*, v. 26, pp. 22-28.

—— (1966*b*). Petrology of the post St. Peter Ordovician, northern Arkansas: *Tulsa Geol. Soc. Digest*, v. 34, pp. 82-98.

FRIEDMAN, G. M. and B. RADKE (1979). Evidence for sabkha overprint and conditions of intermittent emergence in Cambrian-Ordovician carbonates of northeastern North America and Queensland, Australia: *Northeastern Geology*, v. 1., pp. 18-42.

FUCHTBAUER, H. (1972). Influence of salinity on carbonate rocks in the Zechstein Formation, northwestern Germany: *Proc. Hanover Symp. UNESCO, 1968, Geology of Saline Deposits*, pp. 23-31.

GEBELEIN, C. D. and P. HOFFMAN (1973). Algal origin of dolomite laminations in stromatolitic limestone: *Jour. Sed. Petrology*, v. 43, pp. 603-613.

GLENNIE, K. W. (1970). *Desert sedimentary environments:* Dev. in Sedimentology, No. 14, Elsevier, Amsterdam, New York, 222 p.

HANDFORD, C. R. and C. H. MOORE, Jr. (1976). Diagenetic implication of calcite pseudomorphs after halite from the Joachim Dolomite (Middle Ordovician), Arkansas: *Jour. Sed. Petrology*, v. 46, pp. 387-392.

HANSHAW, B. B., W. BACK and R. G. DEIKE (1971). A geochemical hypothesis for dolomitization by groundwater: *Econ. Geology*, v. 66, pp. 710-724.

HAY, R. L. and R. J. MOIOLA (1964). Authigenic silicate minerals in three desert lakes of eastern California: *Geol. Soc. America Sp. Paper 76*, 76 p.

HSU, K. J. and C. SIEGENTHALER (1969). Preliminary experiments on hydrodynamic movement induced by evaporation and their bearing on the dolomite problem: *Sedimentology*, v. 12, pp. 11-25.

JONES, B. F. (1961). Zoning of saline minerals at Deep Spring Lake, California: *U. S. Geol. Survey Prof. Paper 424 B*, pp. 199-209.

KUHNHENN, G. L. and A. V. CAROZZI (1977). Carbonate microfacies of the Platteville Group (Middle Ordovician), Lee and Lasalle Counties, Illinois: *Archives Sciences Genève*, v. 30, pp. 179-212.

LAND, L. S. (1973*a*). Contemporaneous dolomitization of middle Pleistocene reefs by meteoric water, north Jamaica: *Marine Sci. Bull.*, v. 23, pp. 64-92.

—— (1973*b*). Holocene meteoric dolomitization of Pleistocene limestone, north Jamaica: *Sedimentology*, v. 20, pp. 411-424.

MAIKLEM, W. R., D. G. BEBOUT and R. P. GLAISTER (1969). Classification of anhydrite — a practical approach: *Bull. Canadian Petroleum Geology*, v. 17, pp. 194-233.

MANSFIELD, C. F. (1979). Possible biogenic origin for some sedimentary dolomite (abs.): *Am. Assoc. Petroleum Geologists Bull.*, v. 63, p. 490.

MATTES, B. W. and E. W. MOUNTJOY (1980). Burial dolomitization of the Upper Devonian Miette buildup, Jasper National Park, Alberta: in *Concepts and models of dolomitization* (D. H. Zenger, J. B. Dunham and R. L. Ethington, eds.), S.E.P.M. Special Publ. No. 28, pp. 259-297.

MAZZULLO, S. J. (1976). Significance of authigenic K-feldspar in Cambrian-Ordovician carbonate rocks of the Proto-Atlantic shelf in North America: a discussion: *Jour. Sed. Petrology*, v. 46, pp. 1035-1040.

—— and G. M. FRIEDMAN (1977). Competitive algal colonization of peritidal flats in a schizohaline environment: the Lower Ordovician of New York: *Jour. Sed. Petrology*, v. 47, pp. 398-410.

MCKENZIE, J. A., K. J. HSU and J. F. SCHNEIDER (1980). Movement of subsurface waters under the sabkha, Abu Dhabi, UAE, and its relation to evaporative dolomite genesis: in *Concepts and models of dolomitization* (D. H. Zenger, J. B. Dunham and R. L. Ethington, eds.), S.E.P.M. Special Publ. No. 28, pp. 11-30.

MIDDLETON, G. V. (1973). Johannes Walther's Law of the correlation of facies: *Geol. Soc. America Bull.*, v. 81, pp. 979-988.

OKHRAVI, R. (1982). Carbonate microfacies and depositional environments of the Joachim Dolomite (Middle Ordovician), southeast Missouri and southern Illinois, U.S.A.: *Unpubl. Ph. D. thesis, Univ. of Illinois (Urbana-Champaign)*, 141 p.

RUBIN, D. M. and G. M. FRIEDMAN (1977). Intermittently emergent shelf carbonates: an example from the Cambro-Ordovician of eastern New York State: *Sedimentary Geology*, v. 19, pp. 81-106.

SCOTESE, C. R., R. K. BAMBACH, C. BARTON, R. V. D. VOO and A. M. ZIEGLER (1979). Paleozoic base maps: *Jour. Geology*, v. 87, pp. 217-277.

SHEARMAN, D. J. (1966). Origin of marine evaporities by diagenesis: *Inst. Mining Met. Trans.*, v. 75, pp. 208-215.

SLOSS, L. L. (1970). Illinois Basin has deep gas and oil potentials: *World Oil*, v. 170, pp. 59-97.

SOUPAC (1976). Soupac program description, University of Illinois, Urbana-Champaign: *C.S.O.*, v. 1.

STRICKER, G. D. and A. V. CAROZZI (1973). Carbonate microfacies of the Pogonip Group (Lower Ordovician), Arrow Canyon Range, Clark County, Nevada, U.S.A.: *Bull. Centre Rech. Pau-S.N.P.A.*, v. 7, pp. 499-541.

TEMPLETON, J. S. and H. B. WILLMAN (1963). Champlainian Series (Middle Ordovician) in Illinois: *Ill. Geol. Survey Bull.*, 89, 260 p.

THACKER, J. L. and I. R. SATTERFIELD (1978). Guidebook to the geology along Interstate-55 in Missouri: *Report of Investigations Mo. Geol. Survey*, 62, 132 p.

WILLMAN, H. B., E. ATHERTON, E. COLLINSON, J. C. FRYE, M. HOPKINS, E. LINEBACK and J. A. SIMONS (1975). Handbook of Illinois stratigraphy: *Ill. Geol. Survey Bull.*, 95, 261 p.

WOOD, G. V. and M. J. WOLFE (1969). Sabkha cycle in the Arab Darb Formation off the Trucial Coast of Arabia: *Sedimentology*, v. 12, pp. 165-191.

YOUNG, L. M., L. C. FIDDLER and R. W. JONES (1972). Carbonate facies in Ordovician of northern Arkansas: *Am. Assoc. Petroleum Geologists Bull.*, v. 56, pp. 68-80.

ZADNIK, V. E. and A. V. CAROZZI (1963). Sédimentation cyclique dans les dolomies du Cambrien supérieur de Warren County, New Jersey, U.S.A.: *Inst. Nat. Genève Bull.*, v. 62, pp. 1-55.

ZIEGLER, A. M., C. R. SCOTESE, W. S. MCKERROW, M. E. JOHNSON and R. K. BAMBACH (1977). Paleozoic paleogeography: *Annual Rev. Earth Planet. Sci.*, v. 7, pp. 473-502.

PLATE 1

Microfacies 1 trough 4

A. Microfacies 1. Slightly dolomitized (20%) pelletoidal calcisiltite with *Nuia* showing typical fibro-radiated structure with weak pseudo-uniaxial cross. Nicols crossed.

B. Microfacies 1. Dolomitized (65%) calcilutite with abundant bioclasts of *Leperditia*. Note partial replacement of the ostracode tests by medium, euhedral dolomite rhombs. Nicols crossed.

C. Microfacies 2. Dolomitized (50%) matrix-supported intraclastic calcarenite with ostracodes and calcisiltite matrix (now coarse dolomite). Subrounded intraclasts consist of reworked microfacies 1. Nicols crossed.

D. Microfacies 2. Dolomitized (50%) mud-supported intraclastic calcirudite with calcisiltite matrix (now dolomite). Note the pebble-size subangular intraclast which contains a smaller one, *Nuia* and ostracode fragments indicating early submarine lithification and at least two episodes of intraformational reworking. Nicols not crossed.

E. Microfacies 3. Dolomitized (40%) grain-supported intraclastic calcarenite with dolomitized rim cement. Poikilotopic sparite cement filled the cavities after dolomitization of rim cement, bioclasts, and intraclasts. Note the scattered grains of detrital quartz and presence of interparticle porosity (black). Top of the bed is to the left. Nicols crossed.

F. Microfacies 3. Dolomitized (60%) grain-supported intraclastic biocalcarenite with interstitial pelletoidal calcisiltite matrix and poikilotopic sparite cement. Intraclasts and bioclasts (ostracode) are replaced by finely crystalline dolomite rhombs. Nicols crossed.

G. Microfacies 4. Dolomitized (55%) grain-supported intraclastic pelletoidal calcarenite with calcisiltite matrix. Note the intraformational reworking of the desiccation chips which originated from the underlying calcisiltite layer. Scattered grains of bimodal quartz and scoured surface of the calcisiltite layer. Nicols not crossed.

H. Microfacies 4. Dolomitized (55%) grain-supported intraclastic and pelletoidal calcarenite with calcisiltite matrix. Intraclasts consist of the same material as the early cemented underlying dolomitized calcilutite. Desiccation cracks are filled by gypsum and anhydrite cement. Core sample. Nicols crossed.

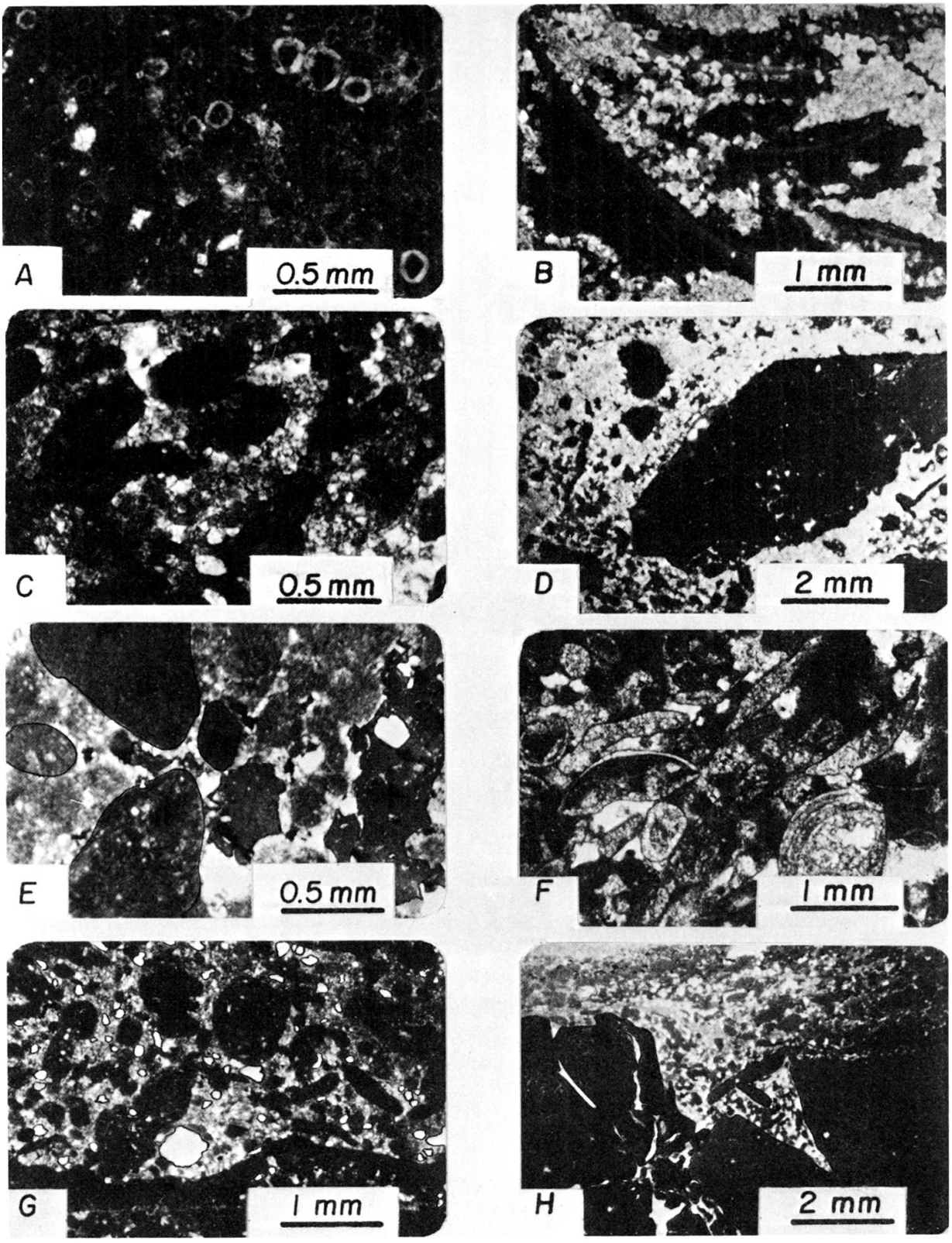
A
0.5 mm
B
1 mm
C
0.5 mm
D
2 mm
E
0.5 mm
F
1 mm
G
1 mm
H
2 mm

PLATE 2

Microfacies 5 through 8

A. Microfacies 5. Highly dolomitized (85%) calcilutite with "L" shaped boring. The groundmass consists of ferroan dolomite, dark spots are organic matter and pyrite. Note the following time relation of the diagenetic events: early lithification of the substratum; boring; deposition of submarine rim cement; complete dolomitization of the rim cement and almost complete dolomitization of interstitial matrix; precipitation of the poikilotopic sparite cement which is stained red by alizarin red S (appearing black) and obliterates the boring porosity. Nicols crossed.

B. Microfacies 5. Dolomitized (45%) calcilutite with interconnected vertical and horizontal borings. The substratum was firm enough to prevent collapsing of the borings which are filled by dolomitized calcilutite matrix, fine detrital quartz and poikilotopic sparite cement. Nicols crossed.

C. Microfacies 6. Finely laminated dolomitized (55%) stromatolites interbedded with dolomitized calcisiltite (light color). Note the desiccation of the upper part of the algal colonies as a result of subaerial exposure. Nicols not crossed.

D. Microfacies 6. Stromatolite (Spongiostromata) surrounded by dolomitized calcilutite matrix. Poikilotopic sparite cement filling the internal void spaces of the organic structure. Nicols not crossed.

E. Microfacies 7. Dolomitized (50%) grain-supported oolitic calcarenite with intercalated thin stromatolitic mats and dolomitized calcisiltite matrix. The cores of the superficial ooids were dissolved giving oomoldic porosity. Some ooids have cavity filling calcite cement in the upper left corner. Nicols crossed + gypsum plate.

F. Microfacies 7. Dolomitized (55%) grain-supported oolitic calcarenite with calcisiltite matrix. Intense compaction of superficial ooids generated spastolites followed by dolomitization and dissolution of their cores giving oomoldic porosity. Note wavy algal intraclasts of stromatolitic micrite in lower left corner. Nicols not crossed.

G. Microfacies 8. Alternating dolomitized (40%) poorly developed dark organic-rich stromatolitic laminae and light colored calcisiltite. White spots are dolomite rhombs. Nicols not crossed.

H. Microfacies 8. Collapse breccia in dolomitized (55%) calcilutite. The cracks are filled by vadose silt and cavity filling poikilotopic sparite cement showing geopetal feature in the lower right corner. Nicols not crossed.

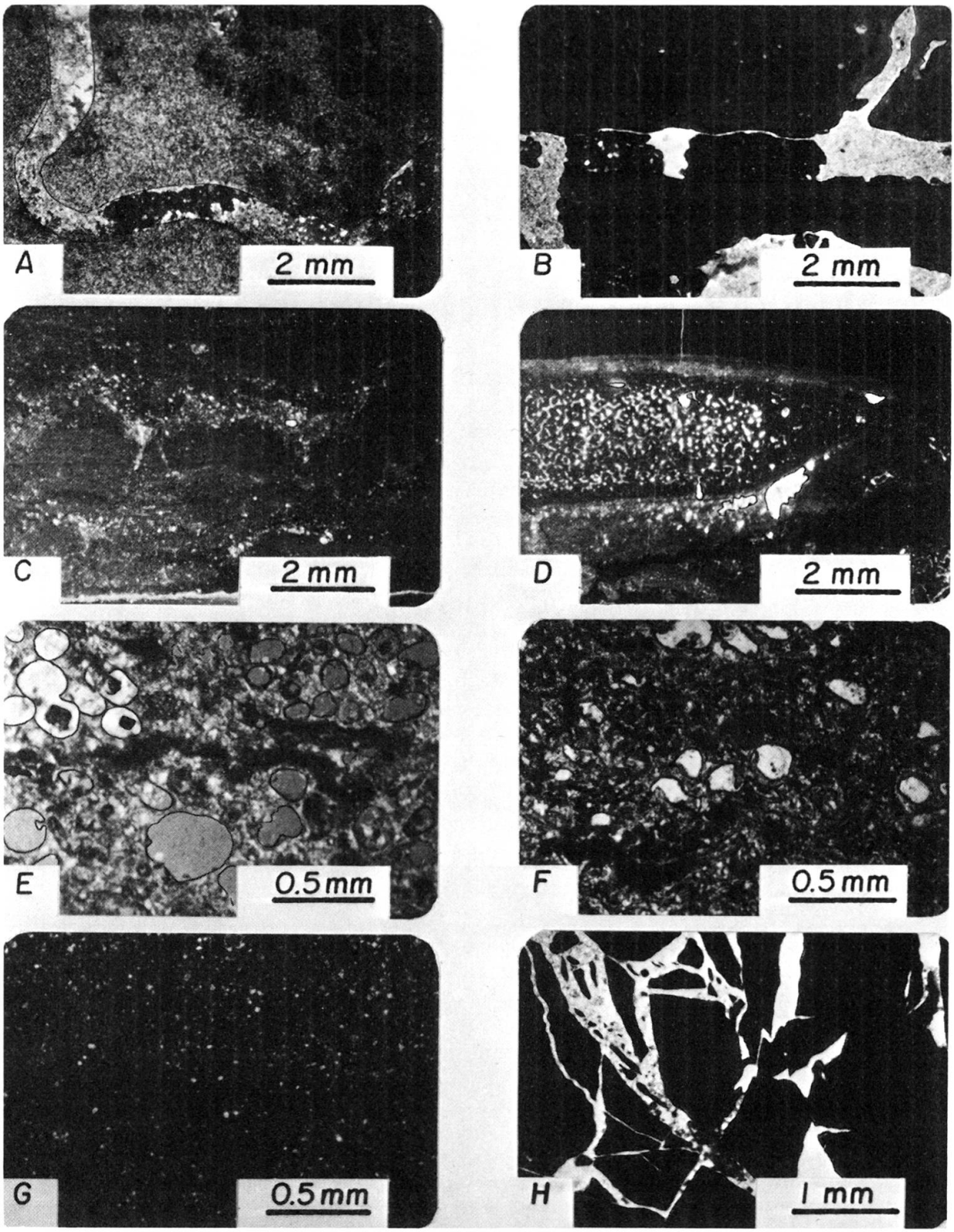
A
2 mm
B
2 mm
C
2 mm
D
2 mm
E
0.5 mm
F
0.5 mm
G
0.5 mm
H
1 mm

PLATE 3

Microfacies 9 through 11

A. Microfacies 9. Dolomitized (45%) pelletoidal calcisiltite with fenestral fabric and bimodal quartz grains. Fenestrae are filled by poikilotopic sparite cement. Vadose silt is present in the upper left corner. Note the marginal replacement of quartz grains. Nicols crossed.

B. Microfacies 9. Hopper-shaped salt cast in dolomitized (50%) calcilutite matrix. Note the preferred growth of corners and edges of the crystal that is typical of hoppers. Nicols crossed + gypsum plate.

C. Microfacies 9. Flat-pebble conglomerate with association of calcisiltite matrix and cavity filling sparite cement. Pebbles resulted from reworking of desiccation chips of the dolomitized calcilutite of microfacies 8. Nicols not crossed.

D. Microfacies 10. Calcite pseudomorphs after nodular-mosaic anhydrite in matrix of dolomitized (45%) calcilutite. Poikilotopic sparite cement associated with vadose silt filling the voids left after dissolution of anhydrite. Outcrop sample (Section C). Nicols crossed.

E. Microfacies 10. Slightly distorted micronodules of mosaic anhydrite with dolomitized (65%) calcilutite matrix showing chickenwire structure. Core sample. Nicols not crossed.

F. Microfacies 11. Bimodal quartz arenite with pressure solution. Rounded and sorted medium grained quartz and feldspar (coarse mode) scattered in a groundmass of fine quartz. Nicols crossed.

G. Microfacies 11. Unimodal quartz arenite with overgrowth. Well sorted and rounded grains of quartz and K feldspar are cemented by overgrowth of respectively same composition. Note the reduced interparticle porosity (black). Nicols crossed.

H. Microfacies 10. Calcite pseudomorph after anhydrite in dolomitized (40%) calcilutite matrix. Cavities are filled by vadose silt and poikilotopic sparite cement. Note the presence of rosettes and single crystals of euhedral authigenic quartz and marginal replacement of authigenic quartz by calcite cement in the lower right center. The precipitation of poikilotopic sparite cement postdated the growth of authigenic quartz. Nicols crossed.

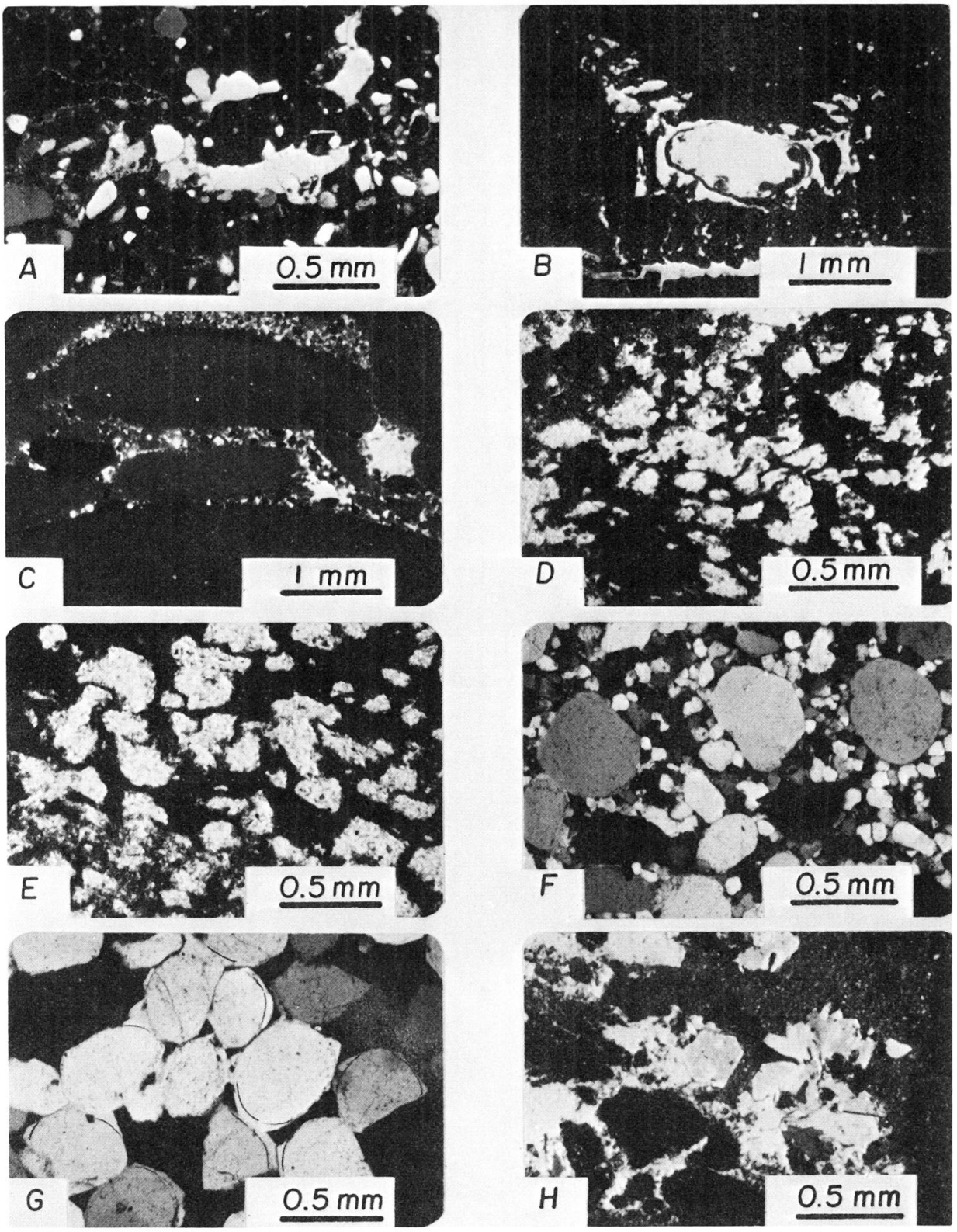
A
0.5 mm
B
1 mm
C
1 mm
D
0.5 mm
E
0.5 mm
F
0.5 mm
G
0.5 mm
H
0.5 mm